Translator's note:

Because the Japanese language does not distinguish singular and plural forms of nouns (e.g. plug vs. plugs), without knowing the exact configuration of the vehicles, often it is difficult to tell whether an item discussed in the report is one or more than one. Please use your judgement when reading the translation below; for example, if a plural noun used in the English translation does not make sense in the context in the view of knowledgeable engineers, probably it is meant to be a singular in the original Japanese text.

Some inconsistencies or discrepancies were found in the Japanese report; e.g. "axle-hub chassis dynamometer" in the description in the text but "chassis dynamometer" in the legend of the corresponding chart. Unless I was certain which was correct, I translated as they are and the English version reflects the inconsistency in the original document.

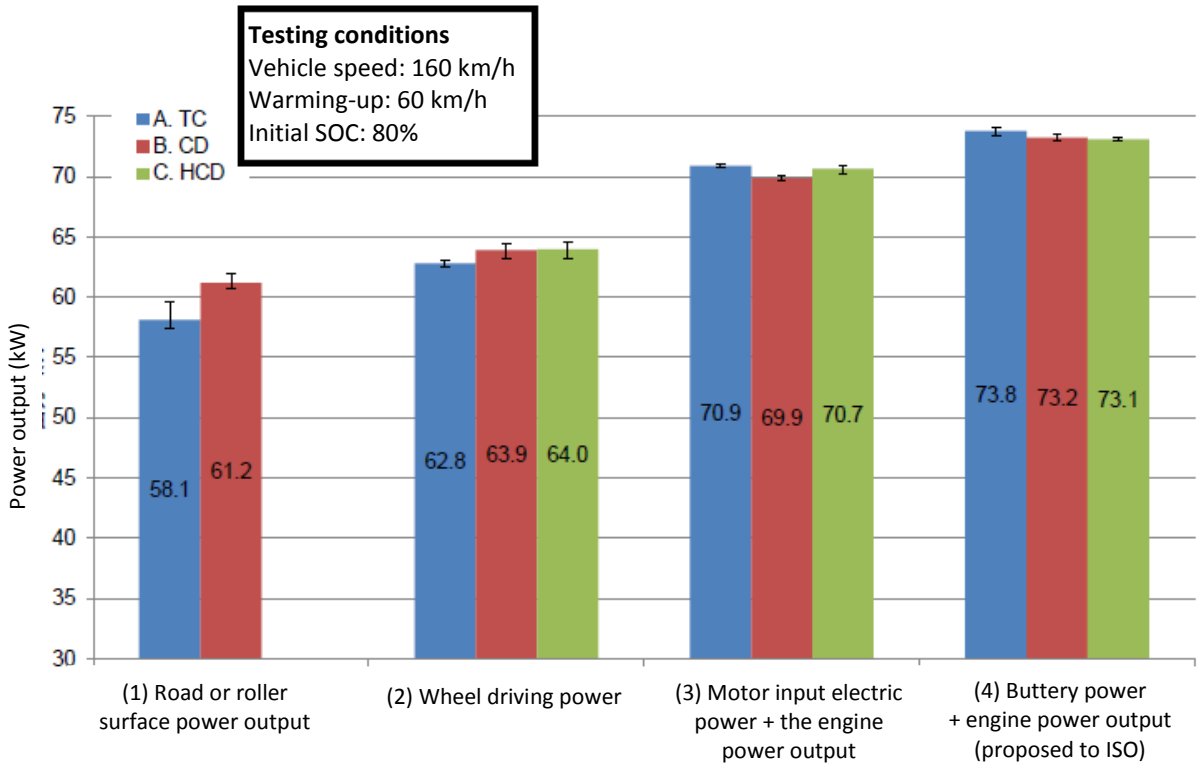

Figure 5.4 Comparison of output measured with different testing facilities (testing vehicle A)

Table 5.1 Comparison of output measured with different testing facilities (testing vehicle A)

	Average value			Deviations		
	A. TC	B. CD	C. HCD	A. TC	B. CD	C. HCD
(1) Road or roller surface	58.1 kW	61.2 kW	–	-0.7 – 1.4 kW	-0.4 – 0.7 kW	–
(2) Wheel driving power	62.8 kW	63.9 kW	64.0 kW	-0.3 – 0.3 kW	-0.8 – 0.5 kW	-0.8 – 0.5 kW
(3) Motor input + engine	70.9 kW	69.9 kW	70.7 kW	-0.1 – 0.1 kW	-0.2 – 0.2 kW	-0.5 – 0.2 kW
(4) Buttery + engine (proposed to ISO)	73.8 kW	73.2 kW	73.1 kW	-0.4 – 0.3 kW	-0.3 – 0.3 kW	-0.1 – 0.1 kW

5.1.3 Testing vehicle B

With testing vehicle B, the effect that differences between three types of facilities have on the measurements of HEV system power output was studied. The on-road test was conducted as shown in Figure 5.5. The test on the chassis dynamometer was conducted as shown in Figure 5.6, and the test with the axle-hub chassis dynamometer was conducted as shown in Figure 5.7. Tests were carried out following the procedure described in section 4.2, and basically by the same methods as with testing vehicle A. The testing speed was decided, considering the specifications of the testing equipment and test results of the effect of speed, to be 89 km/h, which is the speed at which the maximum power is generated in the third gear. Because the vehicle has a stepped transmission, when testing on-road, the gear was shifted down to the third when the speed was 83 km/h, and after accelerating the vehicle full

throttle, at 89 km/h, measurements were taken. When testing on the chassis dynamometer, because the vehicle's driving power is high, taking into consideration slippage of tires, the dynamometer's speed was set at 86 km/h and the vehicle was operated so that the vehicle speed would be 89 km/h at full throttle in the third gear. With the axle-hub chassis dynamometer, since there is no effects such as slippage of tires, the dynamometer's speed was set at 89 km/h. For the SOC, data from the scan tool connected to the diagnostic connector of the vehicle was referred to. The SCO at the beginning of tests was set at 93 per cent, which is considered full charge, but because it is difficult to fully charge the vehicle just before the on-road test, the test was done with the SOC at 65 to 80 per cent.

Figure 5.5 On-road test (testing vehicle B)

Figure 5.6 Chassis dynamometer test (testing vehicle B)

Figure 5.7 Axle-hub chassis dynamometer test (testing vehicle B)

Comparison of results of power output tests of vehicle B conducted with the three facilities is shown in Figure 5.8 and Table 5.2. In the figure and the table, results on real road is marked with “A.TC”, those on the chassis dynamometer are marked with “B.CD”, and those on the axle hub chassis dynamometer are marked with “C.HCD”. The bar chart shows the average value and the range of results of each test repeated four times.

The road surface power output measured on real road was 12.2 kW smaller than the roller surface power output measured in the chassis dynamometer test. One factor that can be pointed out for this is that in the on-road test, measurements are taken during acceleration and test conditions can vary. in the present test, environmental conditions were different, too; in the on-road test, the temperature was 8 ^{o}C and the humidity was 99%, and it is possible that the engine power output was lower due to the effect of the humidity. In addition, there is a difference in friction coefficient on the surface between on road and on a chassis dynamometer, and the effects of tire losses is thought to be different. As for the deviation, the deviation on the chassis dynamometer was -1.9 to 1.6kW, but it was ±7.9 kW on the road, showing a tendency of a large deviation.

With this issue in mind, to avoid effects of tire losses, wheel driving power output was measured. On the road and on the chassis dynamometer, a six-component force meter was used. On the axle hub chassis dynamometer, the power measured by the dynamometer was directly taken as the result. The average power output in the on-road test was approximately 15.4 kW lower than that of the chassis dynamometer and the average power output of the axle hub chassis dynamometer test was 0.7 kW lower than the chassis dynamometer. The difference between the two types of chassis dynamometer was less than 1.0 kW and the effect was small. However, because the measurements taken in the on-road test were greatly different from those from the chassis dynamometer and the axle-hub chassis dynamometer, as in the case of surface power output, it is believed that the main factor is something other than tire loss and some kind of effect is working somewhere more upstream than the wheel power output. Also, compared with the road or roller surface power output, the wheel driving power output was 0.7 kW higher on the road and 3.9 kW higher on the chassis dynamometer, revealing that effects of tire losses are different with different testing facilities. The effect of tire losses on road was very small, which is considered to indicate that the road surface power output was not accurately measured, and it was understood that measuring actual power output on road is difficult. Deviations were -8.6 to 8.5 kW in the on-road test, -1.9 to 1.6 kW in the chassis dynamometer test, and -0.3 to 0.2 kW in the axle hub chassis dynamometer test. These results showed that not only the measurements of the on-road test were lower on average, but also their deviations are very large. As for the deviations of

the chassis dynamometer test, those in the wheel driving outputs were similar to those of roller surface power outputs; switching to the wheel driving power measurements minimally affected the extent of deviations. Since the deviations in the axle-hub chassis dynamometer test were less than 1.0 kW, it is believed that stable measurements can be obtained with an axle-hub chassis dynamometer.

For the comparison with the power of internal combustion engine vehicles, the power output of the vehicle was calculated by adding the motor input electric power and the engine power output, which are further upstream than the transmission gear and the reduction drive. The engine power output is the value derived from the engine power curve and if the throttle is fully open, it can be determined directly based on the rotation speed. For the motor input electric power, the alternating current power between the inverter and the motor was measured. The difference between the chassis dynamometer and the axle-hub chassis dynamometer in the sum of the motor input electric power and the engine power output was 0.1 kW and small, but the value obtained from the on-road test was 2.5 kW smaller than that of the Chassis dynamometer test, showing a difference between the facilities. Deviations were -0.9 to 1.3 kW on the road, ±0.5 kW on the chassis dynamometer and -0.9 to 1.1 kW on the axle hub chassis dynamometer, which were smaller than those of results of wheel driving power output measurements and therefore it is believed that more stable measurements are possible this way.

Further, the power output was calculated as the sum of battery power and the engine power output, which is the method proposed to ISO. For the battery power, the direct current electric power between the battery and the inverter was measured. This sum of battery power and engine power output was, compared with that of chassis dynamometer, 0.8 kW lower on the road and the same on the axle hub chassis dynamometer. Differences among testing facilities were less than 1.0 kW and effects of different facilities were very small. Deviations were -1.6 to 0.9 kW on the road, -0.3 to 0.4 kW on the chassis dynamometer and -0.7 to 1.0 kW on the axle hub chassis dynamometer, and therefore it is believed that more stable measurements are possible, as is the case with the method of adding the motor input electric power and the engine power output.

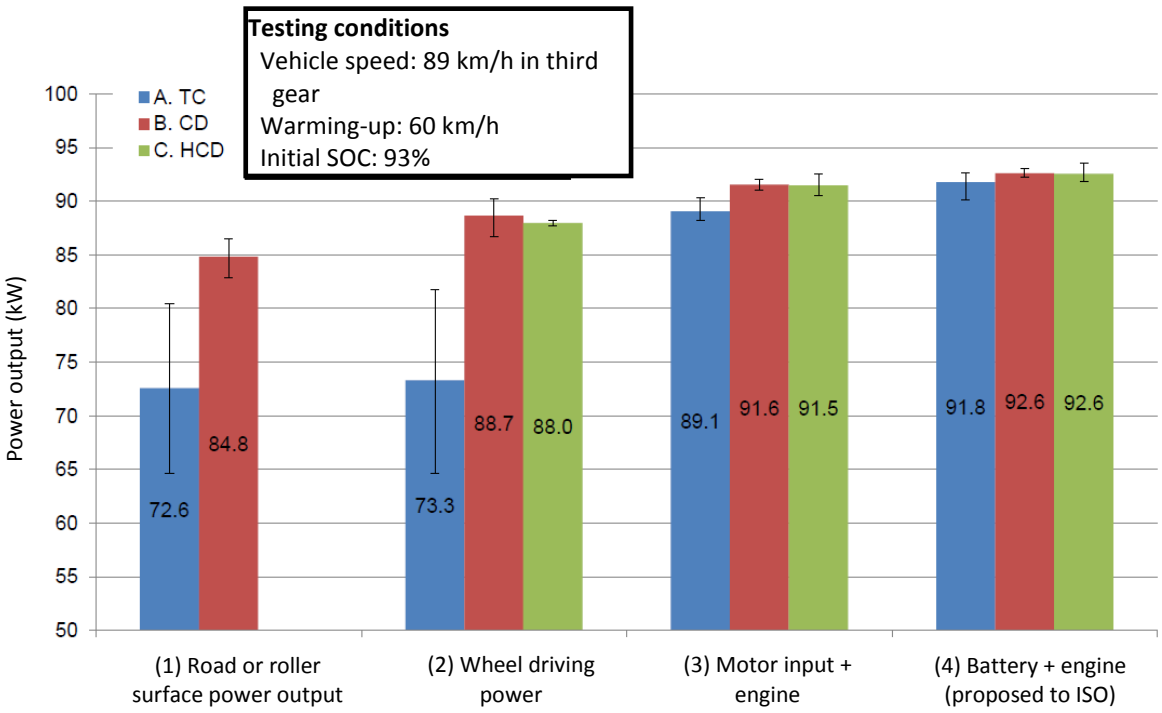

Figure 5.8 Comparison of output measured with different testing facilities (testing vehicle B)

Table 5.2 Comparison of output measured with different testing facilities (testing vehicle B)

	Average value			Deviations		
	A. TC	B. CD	C. HCD	A. TC	B. CD	C. HCD
(1) Road or roller surface	72.6 kW	84.8 kW	–	-7.9 – 7.9 kW	-1.9 – 1.7 kW	–
(2) Wheel driving power	73.3 kW	88.7 kW	88.0 kW	-8.6 – 8.5 kW	-1.9 – 1.6 kW	-0.3 – 0.2 kW
(3) Motor input + engine	89.1 kW	91.6 kW	91.5 kW	-0.9 – 1.3 kW	-0.5 – 0.5 kW	-0.9 – 1.1 kW
(4) Buttery + engine (proposed to ISO)	91.8 kW	92.6 kW	92.6 kW	-1.6 – 0.9 kW	-0.3 – 0.4 kW	-0.7 – 1.0 kW

5.1.4 Testing vehicle C

With testing vehicle C, the effect that differences between three types of facilities have on the measurements of HEV system power output was studied. The on-road test was conducted as shown in Figure 5.9. The test on the chassis dynamometer was conducted as shown in Figure 5.10, and the test with the axle-hub chassis dynamometer was conducted as shown in Figure 5.11. Tests were carried out following the procedure described in section 4.2, but since it is impossible to measure the full-throttle power output while driving at a steady speed on real road, measurements were taken during acceleration. In the tests on the chassis dynamometer and the axle-hub chassis dynamometer, the testing speed was set at 160 km/h, which was given to us by the manufacturer as the speed at which the maximum power output is obtained, but in the on-road test, for the above reason, measurements were taken when the vehicle reached 162 km/h through the full-throttle acceleration from 155 km/h. For the SOC, data from the scan tool connected to the diagnostic connector of the vehicle was referred to. The SCO at the beginning of tests was set at 90 per cent, which is considered full charge, but because it is difficult to precisely adjust the SOC just before the on-road test, it was aimed to have the initial SOC around 90 per cent for the test on the road.

Figure 5.9 On-road test (testing vehicle C)

Figure 5.10 Chassis dynamometer test (testing vehicle C)

Figure 5.11 Axle-hub chassis dynamometer test (testing vehicle C)

Comparison of results of power output tests of vehicle C conducted with the three facilities is shown in Figure 5.12 and Table 5.3. In the figure and the table, results on real road is marked with "A.TC", those on the chassis dynamometer are marked with "B.CD", and those on the axle hub chassis dynamometer are marked with "C.HCD". The bar chart shows the average value and the range of results of each test repeated four times.

The road surface power output measured on real road was 8.0 kW higher than the roller surface power output measured in the chassis dynamometer test. One factor that can be pointed out for this is that in the on-road test, measurements were taken during acceleration and therefore testing conditions are different, and issues of acceleration in measurements possibly exist as well. In addition, there is a difference in friction coefficient on the surface on road and on a chassis dynamometer and the effects of tire losses are thought to be different. As for the deviation, the maximum deviation on the chassis dynamometer was approximately 0.4 kW, but it was around 2.7 KW on the road. The difference in the degrees of deviations is expected to be studied by the HEV System Power Working Group of JARI in the future, but the minimum display unit for the operations of the tests is thought to be one kW. In that

case, the precision required is thought to be at least one kW or smaller. Considering this, the deviations in the road surface power output are thought to be large.

With this issue in mind, to avoid effects of tire losses, wheel driving power output was measured. On the road and on the chassis dynamometer, a six-component force meter was used. On the axle hub chassis dynamometer, the power measured by the dynamometer was directly taken as the result. The power output measured in the on-road test was approximately the same as the chassis dynamometer test, and the power output in the axle hub chassis dynamometer test was 5.4 kW higher than that of the chassis dynamometer test. Also, compared with the road or roller surface power output, the wheel driving power output was 0.3 kW lower on the road and 13.4 kW higher on the chassis dynamometer, revealing that effects of tire losses are different with different testing facilities. Based on the comparison with driving power output measured on the axle-hub chassis dynamometer, it is believed that the surface power output in the on-road test and the wheel driving power output in the chassis dynamometer test were not accurately measured. Deviations were -4.3 to 3.7 kW in the on-road test, and -1.3 to 0.8 kW in the chassis dynamometer, both of which were worse than those in the road or roller surface measurements; measuring wheel driving power output was not effective to reduce the effects of tire losses. The axle hub chassis dynamometer test resulted in -0.7 kW to 0.6 deviations, but they are smaller than 1.0 kw, and it is believed that stable measurements are possible with the axle-hub chassis dynamometer.

For the comparison with the power of internal combustion engine vehicles, the power output of the vehicle was calculated by adding the motor input electric power and the engine power output, which are further upstream than the transmission gear and the reduction drive. The engine power output is the value derived from the engine power curve and if the throttle is fully open, it can be determined directly based on the rotation speed. For the motor input electric power, the alternating current power between the inverter and the motor was measured. The sum of the motor input electric power and the engine power output was 0.4 kW lower on the road than on the chassis dynamometer and 1.4 kW higher on the axle hub chassis dynamometer than on the chassis dynamometer. Differences among testing facilities were around 1.0 kW, which means effects of different facilities were small. Deviations were -0.9 to 0.7 kW on the road, -0.4 to 0.6 kW on the chassis dynamometer and -0.1 to 0.2 kW on the axle hub chassis dynamometer, which were smaller than those of results of wheel driving power output measurements and therefore it is believed that stable measurements are possible this way.

Further, the power output was calculated as the sum of battery power and the engine power output, which is the method proposed to ISO. For the battery power, the direct current electric power between the battery and the inverter was measured. This sum of battery power and engine power output was, 0.9 kW lower on the road compared than the chassis dynamometer, and it was the same between the chassis dynamometer and the axle hub chassis dynamometer. Differences among testing facilities were less than 1.0 kW and effects of different facilities were very small. Deviations were -0.5 to 0.3 kW on the road, ±0.2 kW on the chassis dynamometer and ±0.2 kW on the axle hub chassis dynamometer, and therefore it is believed that stable measurements are possible.

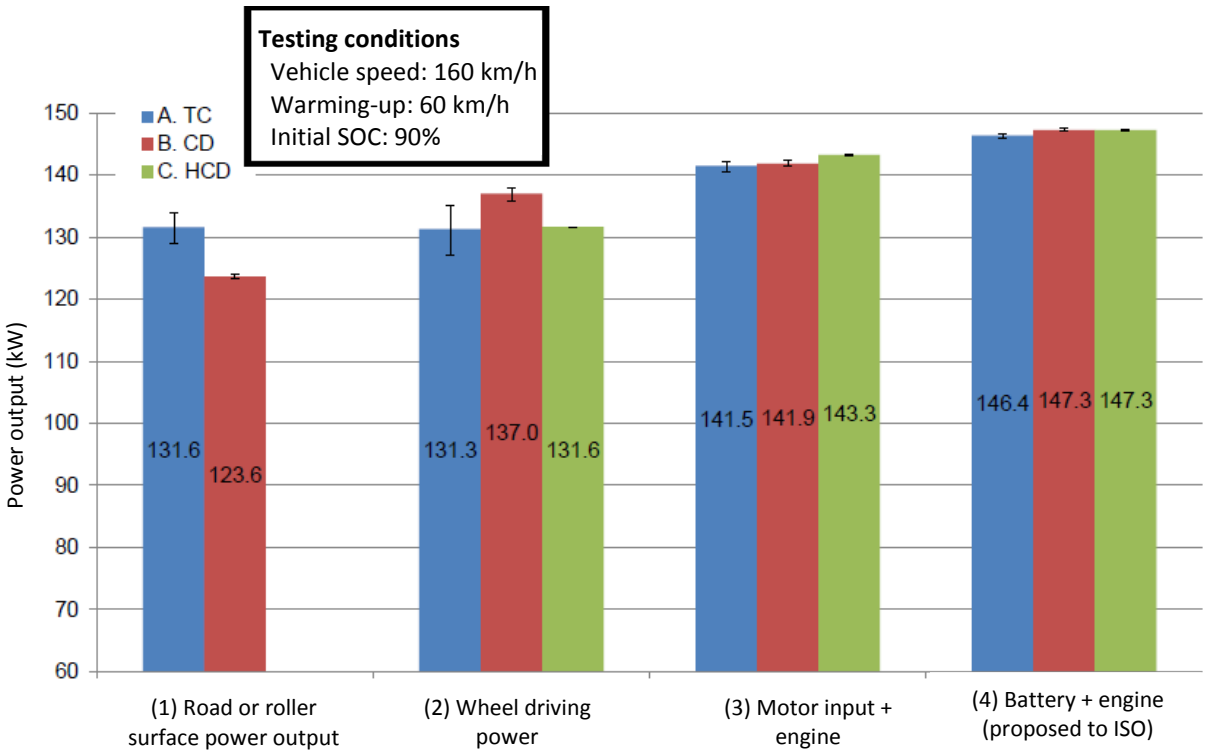

Figure 5.12 Comparison of output measured with different testing facilities (testing vehicle C)

Table 5.3 Comparison of output measured with different testing facilities (testing vehicle C)

	Average value			Deviations		
	A. TC	B. CD	C. HCD	A. TC	B. CD	C. HCD
(1) Road or roller surface	131.6 kW	123.6 kW	–	-2.7 – 2.5 kW	-0.3 – 0.4 kW	–
(2) Wheel driving power	131.3 kW	137.0 kW	131.6 kW	-4.3 – 3.7 kW	-1.3 – 0.8 kW	-0.7 – 0.6 kW
(3) Motor input + engine	141.5 kW	141.9 kW	143.3 kW	-0.9 – 0.7 kW	-0.4 – 0.6 kW	-0.1 – 0.2 kW
(4) Buttery + engine (proposed to ISO)	146.4 kW	147.3 kW	147.3 kW	-0.5 – 0.3 kW	-0.2 – 0.2 kW	-0.2 – 0.2 kW

5.1.5 Summary

Considering that different testing facilities and different locations where measurements are taken can affect replicability of maximum power measurement results, a study was conducted using three types of facilities: real road, chassis dynamometer and axle-hub chassis dynamometer. Deviations were used as the basis of evaluation of replicability. Regarding how the degrees of deviations should be judged, the HEV System Power Working Group of JARI is expected to study in the future, but the minimum display unit for the operations of the tests is thought to be one kW. In that case, the precision required is thought to be at least one kW or smaller. Among the three testing facilities, values obtained were different due to effects such as tire loss depending on where measurements are taken. Differences of

power output measurements among facilities were reviewed and their factors and solutions were studied. The comparative results are shown in Table 5.4.

The maximum deviation of road surface power outputs measured on road was 1.4 kW with testing vehicle A, 7.9 kW with testing vehicle B and 2.7 kW with testing vehicle C. Possible factors for the measuring errors include errors due to measuring during acceleration, tire losses and testing temperature. Since environmental factors cannot be improved, in order to exclude tire losses and errors due to measuring during acceleration, wheel driving power output was measured. Resulting maximum deviations were 0.3 kW with testing vehicle A, 8.9 kW with testing vehicle B, and 4.3 kW with testing vehicle C. While the deviations decreased with testing vehicle A, there was no effect found with testing vehicles B and C, and it is believed that other factors are causing deviations. When the HEV system power output was calculated by adding the engine power output and the battery power, which is the method proposed to the ISO, the maximum deviation with testing vehicle A was 0.4 kW, which is not significantly different from that in the wheel driving power measurements, but with testing vehicle B, the maximum deviation was 1.6 kW and it was -0.5 kW with testing vehicle C, which are significantly smaller, and stable measurements were deemed possible this way.

Next, when roller surface power outputs were measured on the chassis dynamometer, the maximum deviation was 0.7 kW with testing vehicle A, 1.9 kW with testing vehicle B and 0.4 kW with testing vehicle C, indicating that relatively stable measurements were possible. A conceivable factor of the measurement errors was the effect of tire losses. To eliminate errors caused by tire losses, wheel driving power outputs were measured. The results showed a maximum deviation of 0.8 kW with testing vehicle A, 1.9 kW with testing vehicle B and 1.3 kW with testing vehicle C. Because these did not show any effect on deviations, it is believed that other factors affect measurements. Further, when the HEV system power output was measured by the method proposed to the ISO, deviations were significantly reduced; the maximum deviation with testing vehicle A was 0.3 kW, 0.4 kW with testing vehicle B and 0.2 kW with testing vehicle C. Stable measurements were deemed possible by this method.

In the measurements of wheel driving power outputs taken with the axle-hub chassis dynamometer, the largest deviations were 0.8 kW with testing vehicle A, 0.3 kW with testing vehicle B, and 0.7 kW with testing vehicle C, which showed that relatively stable measurements were possible. When the system power outputs were calculated by the method proposed to the ISO, the largest deviations were 0.1 kW with testing vehicle A, 1.0 kW with testing vehicle B, and 0.2 kW with testing vehicle C. This made it clear that stable measurements can be obtained this way.
It is understood, based on the above results, that by measuring HEV system power outputs by the method proposed to the ISO with a chassis dynamometer or an axle-hub chassis dynamometer, deviations can be limited to one kW or smaller. It is believed that when HEV system power output is calculated by this method, because the engine power output calculated based on the engine's rotation speed and measurements of the battery power are directly used, varying losses that occur in tires or the transmission do not affect the values and therefore stable measuring results are possible.

Table 5.4 Effects of facilities on power measurements of HEV systems

		Real road			Chassis dynamometer			Axle-hub chassis dynamometer		
Tested vehicle		A	B	C	A	B	C	A	B	C
Road surface power output (real road)	Average measurement of HEV system power	58.1 kW	72.6 kW	131.6 kW	61.2 kW	84.8 kW	123.6 kW	–	–	–
	Power measured	Acceleration			Power output on chassis dynamometer			–		
Roller surface power output (chassis dynamometer)	Deviation	-0.7 – 1.4 kW (-1.2 – 2.4%)	-7.9 – 7.9 kW (-10.9 – 10.9%	-2.7 – 2.5 kW (-2.1 – 1.9%)	-0.4 – 0.7 kW (-0.7 – 1.1%)	-1.9 – 1.7 kW (-2.2 – 2.0%	-0.3 – 0.4 kW (-0.2 – 0.3%)	–	–	–
	Contributing factors to errors	Tire losses, testing environment, acceleration measurement			Tire losses			–		
Wheel-driving power	Error-alleviating measures	Wheel torque measurement; others issues are hard to deal with			Wheel torque measurement			–		
	Average measurement of HEV system power	62.8 kmW	73.3 kW	131.3 kW	63.9 kW	88.7 kW	137.0 kW	64.0 kW	88.0 kW	131.6 kW
	Power measured	Wheel-driving power			Wheel-driving power			Power output on axle-hub chassis dynamometer		
	Deviation	-0.3 – 0.3 kW (-0.5 – 0.5%)	-8.6 – 8.5 kW (-11.7 – 11.6%	-4.3 – 3.7 kW (-3.3 – 2.8%)	-0.8 – 0.5 kW (-1.3 – 0.8%)	-1.9 – 1.6 kW (-2.1 – 1.8%	-1.3 – 0.8 kW (-0.9 – 0.6%)	-0.8 – 0.5 kW (-1.3 – 0.8%)	-0.3 – 0.2 kW (-0.3 – 0.2%	-0.7 – 0.6 kW (-0.5 – 0.5%)
Method proposed to ISO	Average measurement of HEV system power	73.8 kW	91.8 kW	146.4 kW	73.2 kW	92.6 kW	147.3k W	73.1 kW	92.6 kW	147.3 kW
	Power measured	Engine + battery			Engine + battery			Engine + battery		
	Deviation	-0.4 – 0.3 kW (-0.5 – 0.4%)	-1.6 – 0.9 kW (-1.7 – 1.0%	-0.5 – 0.3 kW (-0.3 – 0.2%)	-0.3 – 0.3 kW (-0.4 – 0.4%)	-0.3 – 0.4 kW (-0.3 – 0.4%)	-0.2 – 0.2 kW (-0.1 – 0.1%)	-0.1 – 0.1 kW (-0.2 – 0.2%)	-0.7 – 1.0 kW (-0.8 – 1.1%	-0.2 – 0.2 kW (-0.1 – 0.1%)

5.2 Measurement of operating conditions of HEV systems at the time of maximum power output

5.2.1 Overview of the tests

Whether or not measurements that are necessary to determine operating conditions of engine, motor and battery at the time of maximum power output can be taken the same way on differently-structured

HEV systems without significantly modifying the vehicles was examined. Where some measurements could not be taken, whether or not operating conditions could be determined based only on measurements that could be obtained was studied. Where operating conditions could be determined, the differences between the calculated HEV system power based on those measurements and the manufacturers' listed power values were reviewed.

5.2.2 Measured items and measuring locations of testing vehicle A

Table 5.5 shows items measured, their measuring locations, measuring methods and devises used for measurement (manufacturers of the devices, model number, etc.) regarding testing vehicle A. Figure 5.13 shows measuring devices installed in the interior of the vehicle.

To determine the operating conditions of the engine, the rotational speed and the load are required. For the engine rotational speed, the rotational speed of the crank pulley was measured. For the engine load, while the torque cannot be directly measured, measurements such as the throttle opening rate, the intake pipe pressure and the fuel flow rate can be used as replacements. Because the throttle of the testing vehicle is electronically controlled, its opening rate could not be measured from outside. As shown in Figure 5.14, the intake pipe pressure was measured by splitting the genuine piping. To measure the fuel flow rate, the genuine pipe was extended and a flowmeter was inserted in the fuel line. In addition, to verify the replicability of the test, the engine water temperature, the engine oil temperature and the temperature of the air surrounding the engine were measured. As shown in Figure 5.15, the engine water temperature was measured by inserting a pipe in the genuine engine cooling water hose. The engine oil temperature was, as shown in Figure 5.16, measured with a thermocouple affixed to the oil level gauge.

To determine operating conditions of the motor, measurements such as the motor rotational speed and the torque are necessary, but they cannot be directly measured because the motor is installed inside the transmission. For this reason, as shown in Figure 5.17, the AC voltage and the electronic current, which are input to the motor, were measured. Both could be measured since in testing vehicle A the inverter and the motor are connected with cables. Also, because the motor is cooled with the oil cooling system that uses the ATF, as shown in Figure 5.18, the oil drain plug was modified and the ATF temperature was measured.

With regard to the inverter, the DC voltage and the electronic current, which are the input to the inverter, were measured. Because the inverter's cooling system is water-based, as shown in Figure 5.19, a pipe was inserted into the genuine cooling water hose and the temperature of the cooling water was measured.

With regard to the battery, the DC electric current, which is the output, was measured. Since the voltage is the same as the input voltage of the inverter, it was skipped with the battery. The battery surface temperature was measured, as shown in Figure 5.20, at three locations, which is the same number as the genuine system, near the genuine temperature sensors' installation spots. To determine the temperature of the battery cooling air flow, as shown in Figure 5.21, the temperature at the air intake port was measured, as well as the exit temperature to be used as the air temperature after the cooling, as shown in Figure 5.22.

As the vehicle's driving power, the wheel driving power was measured. As shown in Figure 5.23, a six-component force meter was installed on the right and left sides of the driving wheels. To measure the vehicle's acceleration, as shown in Figure 5.24, an accelerometer was installed near the centre of the vehicle's body.

Table 5.5 Measurements taken of the testing vehicle A

Item	Name	Location	Method	Name of devise used for measurement
Engine	Engine rotational speed	Crank pulley	Optical sensor	Keyence FS-V21
	Throttle opening rate	Measurement not possible		
	Intake pipe pressure	Vacuum hose	Vacuum gauge	Keyence AP-44
	Fuel flow rate	Entrance of engine	Fuel flowmeter	Ono Sokki FP-213S
	Fuel temperature	Entrance of engine	Sheathed thermocouple	Type T
	Water temperature	Exit of engine	Sheathed thermocouple	Type T
	Intake air temperature	Air cleaner	Thermocouple	Type T
	Oil temperature	Level gauge	Sheathed thermocouple	Type T
	Air temperature around engine	Above engine	Thermocouple	Type T
Motor	Motor rotational speed	Measurement not possible		
	Motor input voltage (AC)	Inside inverter	Wattmeter	Hioki E.E. Corp. 3194
	Motor input electric current (AC)	Exit of inverter	Clamp meter	Hioki E.E. Corp. 9278 x 3
	ATF temperature	Transmission drain	Sheathed thermocouple	Type T
Inverter	Inverter input voltage (DC)	Inside inverter	Wattmeter	Hioki E.E. Corp. 3194
	Inverter cooling water temperature	Exit of inverter	Sheathed thermocouple	Type T
	Inverter input electronic current (DC)	Entrance of inverter	Clamp meter	Hioki E.E. Corp. 9278
Battery	Battery electronic current	Exit of battery	Clamp meter	Hioki E.E. Corp. 9278
	Battery surface temperature	Surface of battery	Thermocouple	Type T x 3
	Battery cooling air temperature	Intake port of cooling air	Thermocouple	Type T
	Air temperature after cooling battery	Exit of cooling air	Thermocouple	Type T
Vehicle	Wheel driving power on left	Wheel	Six-component force meter	Kyowa Electronic Instruments WFT-B-8KNSB13
	Wheel driving power on right	Wheel	Six-component force meter	
	Roller driving power	Chassis dynamometer	Load cell	–
	Wheel rotational speed on left	Wheel	Six-component force meter	Kyowa Electronic Instruments WFT-B-8KNSB13
	Wheel rotational speed on right	Wheel	Six-component force meter	
	Vehicle speed	Interior (on-road test)	GPS vehicle speedometer	Vios System VGVS-SP5Ci
		Chassis dynamometer	Chassis dynamometer	Meidensha

		(chassis dynamometer test)		
	Vehicle acceleration	Interior	Accelerometer	Kyowa Electronic Instruments AS-1TG

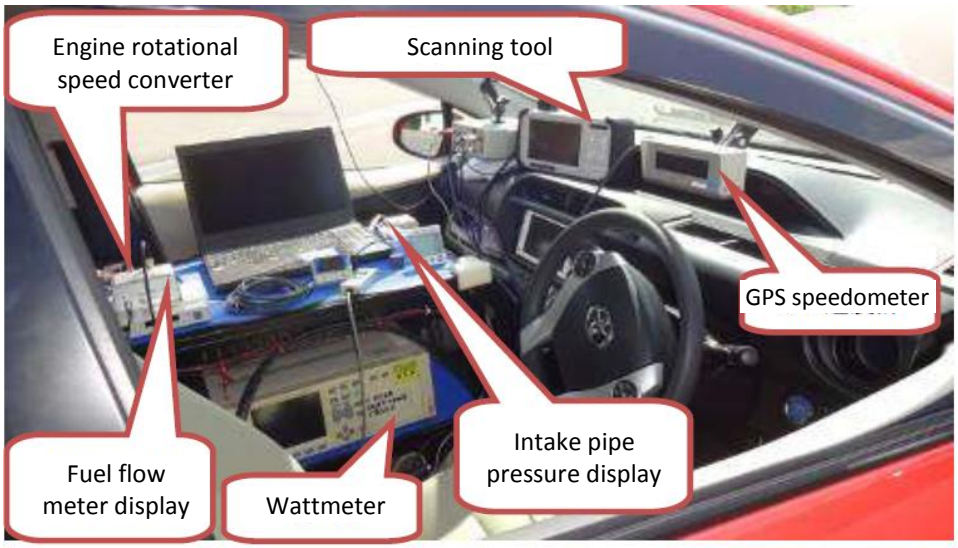

Figure 5.13 Measuring devices in the interior (testing vehicle A)

Figure 5.14 Measuring location of intake pipe pressure (testing vehicle A)

Figure 5.15 Measuring location of engine cooling water temperature
(testing vehicle A)

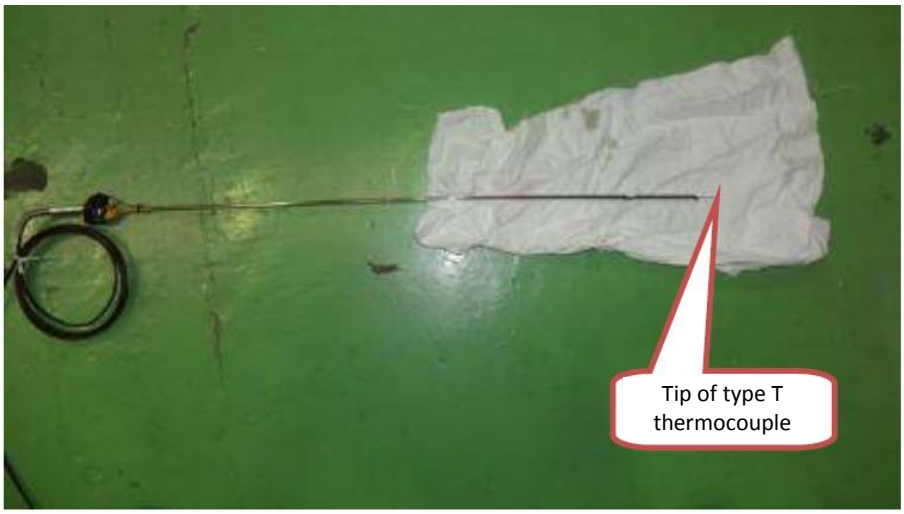

Figure 5.16 Measuring location of engine oil temperature
(testing vehicle A)

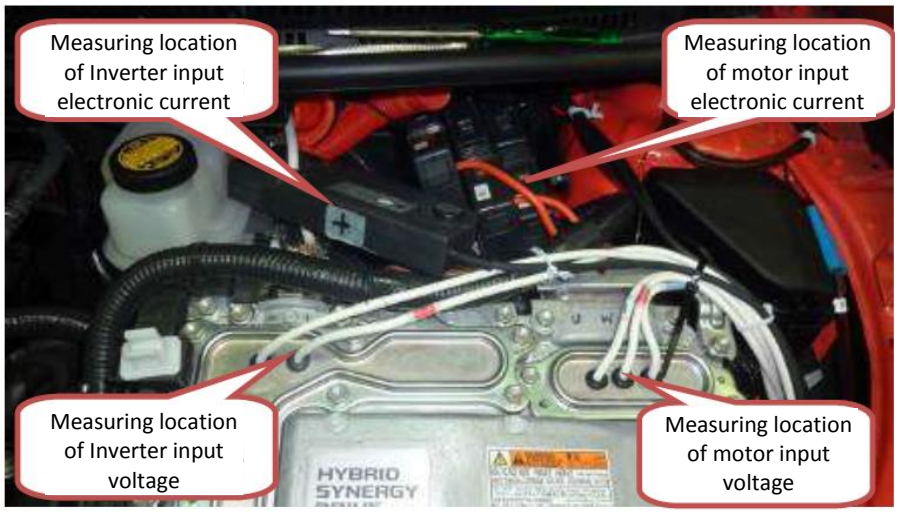

Figure 5.17 Measuring locations of input voltage and electric current of inverter and motor (testing vehicle A)

Figure 5.18 Measuring location of ATF temperature (testing vehicle A)

Figure 5.19 Measuring location of inverter cooling water temperature (testing vehicle A)

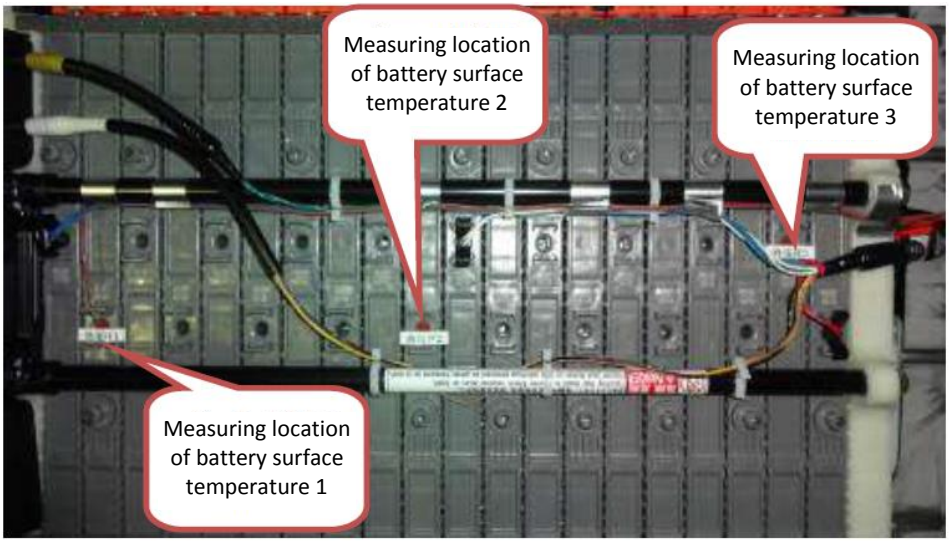

Figure 5.20 Measuring location of battery surface temperature (testing vehicle A)

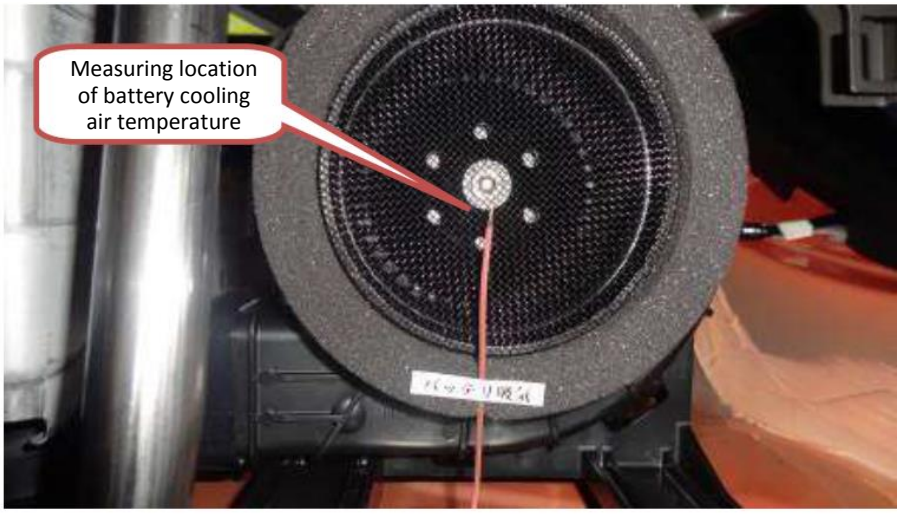

Figure 5.21 Measuring location of battery cooling air temperature (testing vehicle A)

Figure 5.22 Measuring location of temperature after cooling battery (testing vehicle A)

Figure 5.23 Measuring location of wheel driving power (testing vehicle A)

Figure 5.24 Measuring locations of acceleration (testing vehicle A)

5.2.3 Measured items and measuring locations of testing vehicle B

Table 5.6 shows items measured, their measuring locations, measuring methods and devises used for measurement (manufacturers of the devices, model number, etc.) regarding testing vehicle B. Figure 5.25 shows measuring devices installed in the interior of the vehicle.

To determine the operating conditions of the engine, the rotational speed and the load are required. For the engine rotational speed, the rotational speed of the crank pulley was measured as shown in Figure 5.26. For the engine load, while the torque cannot be directly measured, measurements such as the throttle opening rate, the intake pipe pressure and the fuel flow rate can be used as replacements. Because the throttle of the testing vehicle is electronically controlled, its opening rate could not be measured from outside. The intake pipe pressure was measured by splitting the genuine piping. As

shown in Figure 5.27, to measure the fuel flow rate, the genuine pipe was extended and a flowmeter was inserted in the fuel line. In addition, to verify the replicability of the test, the engine water temperature, the engine oil temperature and the temperature of the air surrounding the engine were measured. The engine water temperature was measured by inserting a pipe in the genuine engine cooling water hose. The engine oil temperature was measured with a thermocouple affixed to the oil level gauge.

To determine operating conditions of the motor, measurements such as the motor rotational speed and the torque are necessary, but they cannot be directly measured because the motor is installed inside the transmission. For this reason, as shown in Figure 5.28, the AC voltage and the electronic current, which are input to the motor, were measured. Both could be measured since in testing vehicle B the inverter and the motor are connected with cables. Also, because the motor is cooled with the oil cooling system that uses the ATF, the oil drain plug was modified and the ATF temperature was measured.

With regard to the inverter, the DC voltage, which is the input to the inverter, was measured. Because the inverter's cooling system is air-based, as shown in Figure 5.29, the temperature near the cooling fan of the inverter was measured.

With regard to the battery, the service plug was modified and the DC electric current was measured. Since the voltage is the same as the input voltage of the inverter, it was skipped with the battery. The battery surface temperature was measured, as shown in Figure 5.30, at four locations, which is the same number as the genuine system, near the genuine temperature sensors' installation spots. To determine the temperature of the battery cooling air flow, as shown in Figure 5.31, the temperature at the air intake port was measured, as well as the exit temperature to be used as the air temperature after the cooling, as shown in Figure 5.32.

As the vehicle's driving power, the wheel driving power was measured. As shown in Figure 5.33, a six-component force meter was installed on the right and left sides of the driving wheels. To measure the vehicle's acceleration, an accelerometer was installed near the centre of the vehicle's body.

Table 5.6 Measurements taken of the testing vehicle B

Item	Name	Location	Method	Name of devise used for measurement
Engine	Engine rotational speed	Crank pulley	Optical sensor	Keyence FS-V21
	Throttle opening rate	Measurement not possible		
	Intake pipe pressure	Vacuum hose	Vacuum gauge	Keyence AP-44
	Fuel flow rate	Entrance of engine	Fuel flowmeter	Ono Sokki FP-213S
	Fuel temperature	Entrance of engine	Sheathed thermocouple	Type T
	Water temperature	Exit of engine	Sheathed thermocouple	Type T
	Intake air temperature	Air cleaner	Thermocouple	Type T
	Oil temperature	Level gauge	Sheathed thermocouple	Type T
	Air temperature around engine	Above engine	Thermocouple	Type T
Motor	Motor rotational speed	Measurement not possible		
	Motor input voltage (AC)	Top of inverter	Wattmeter	Hioki E.E. Corp. 3194

	Motor input electric current (AC)	Bottom of vehicle	Clamp meter	Hioki E.E. Corp. 9278 x 3
	ATF temperature	Transmission drain	Sheathed thermocouple	Type T
Inverter	Inverter input voltage (DC)	Top of inverter	Wattmeter	Hioki E.E. Corp. 3194
	Inverter temperature	Exit of inverter	Sheathed thermocouple	Type T
Battery	Battery electronic current	Service plug	Clamp meter	Hioki E.E. Corp. 9278
	Battery surface temperature	Surface of battery	Thermocouple	Type T x 4
	Battery cooling air temperature	Intake port of cooling air	Thermocouple	Type T
	Temperature after cooling battery	Exit of cooling air	Thermocouple	Type T
Vehicle	Wheel driving power on left	Wheel	Six-component force meter	Kyowa Electronic Instruments WFT-B-8KNSB13
	Wheel driving power on right	Wheel	Six-component force meter	
	Roller driving power	Chassis dynamometer	Load cell	–
	Wheel rotational speed on left	Wheel	Six-component force meter	Kyowa Electronic Instruments WFT-B-8KNSB13
	Wheel rotational speed on right	Wheel	Six-component force meter	
	Vehicle speed	Interior (on-road test)	GPS vehicle speedometer	Vios System VGVS-SP5Ci
		Chassis dynamometer (chassis dynamometer test)	Chassis dynamometer	Meidensha
	Vehicle acceleration	Interior	Accelerometer	Kyowa Electronic Instruments AS-1TG

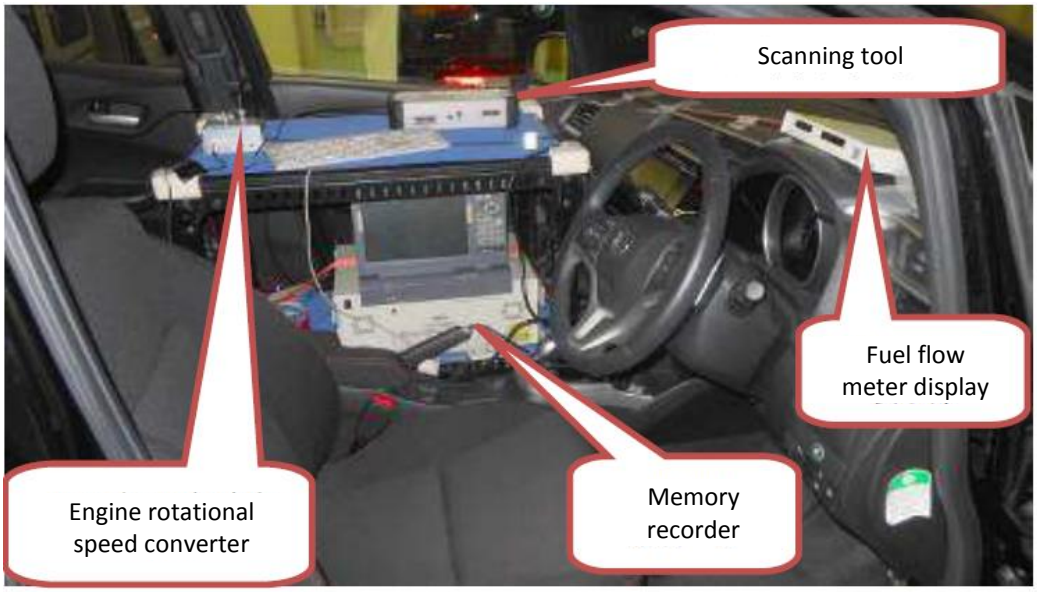

Figure 5.25 Measuring devices in the interior (testing vehicle B)

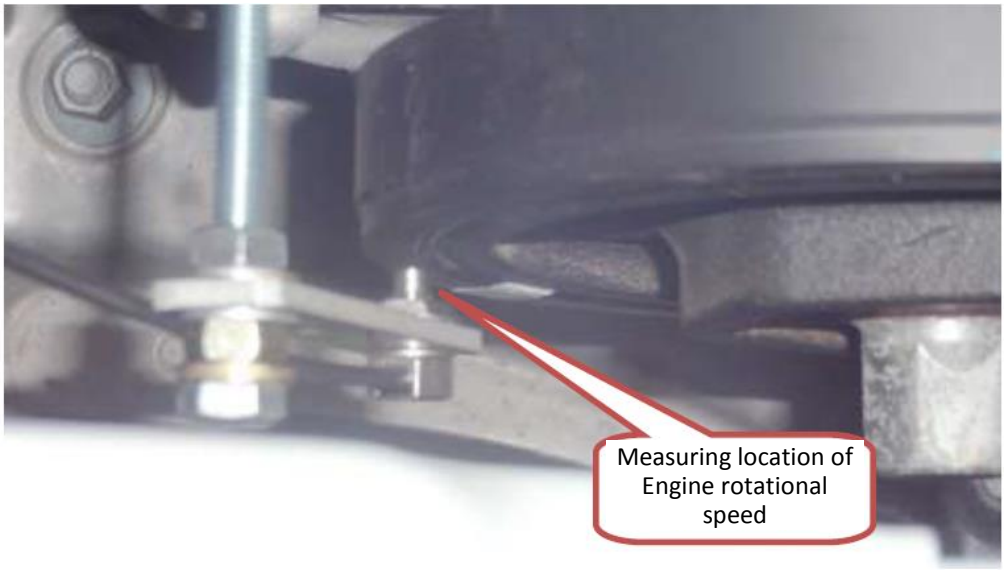

Figure 5.26 Measuring location of engine rotational speed (testing vehicle B)

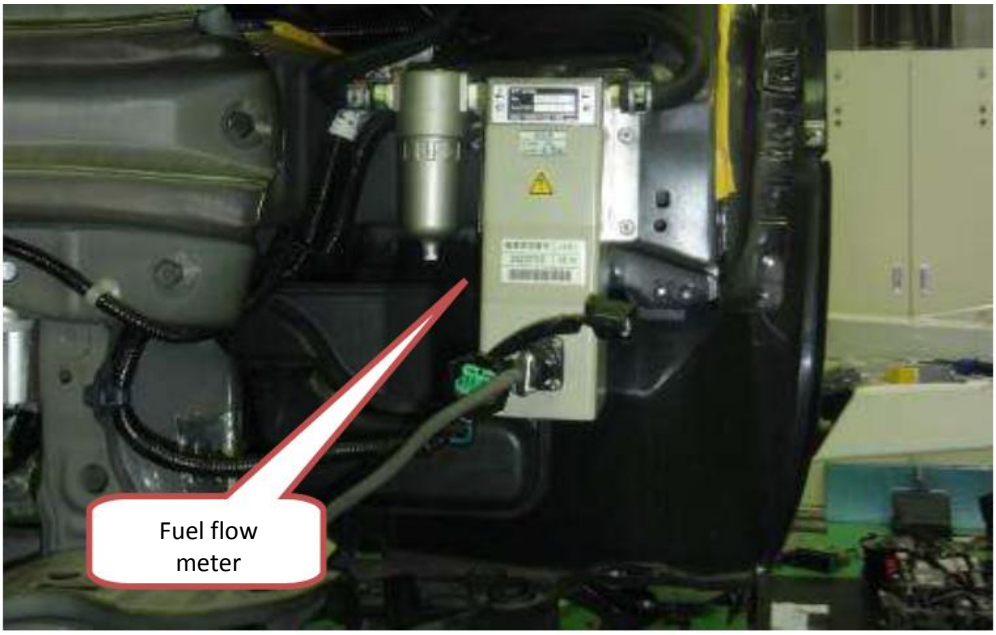

Figure 5.27 Measuring location of fuel flow rate (testing vehicle B)

Figure 5.28 Measuring location of inverter input electric current (testing vehicle B)

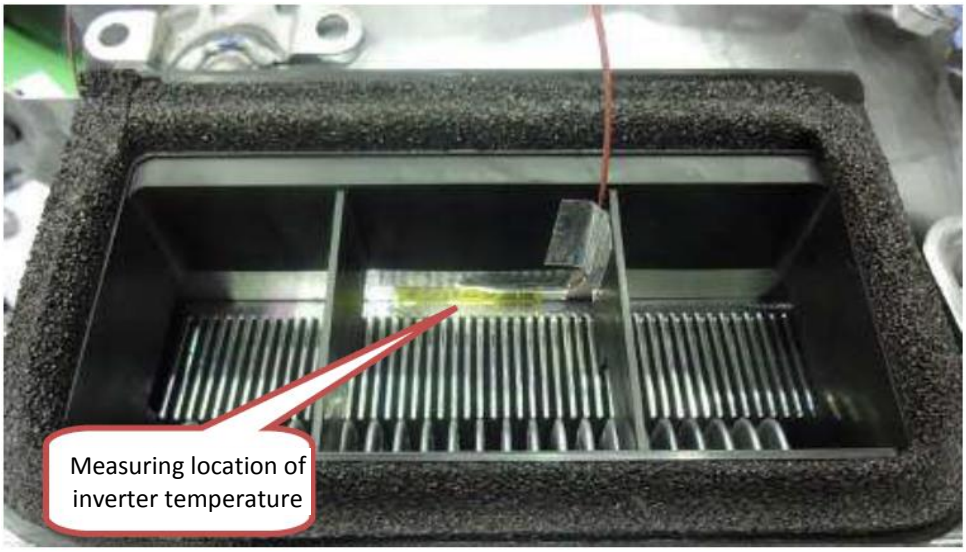

Figure 5.29 Measuring location of inverter temperature (testing vehicle B)

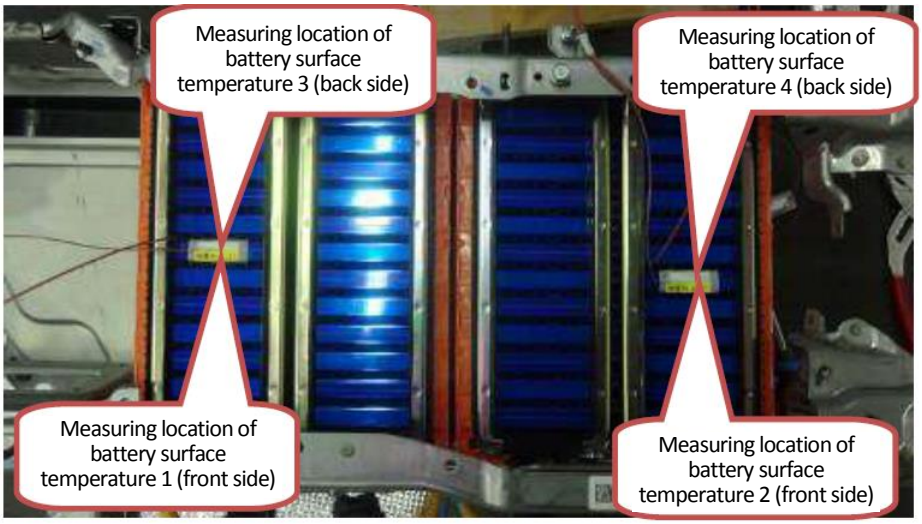

Figure 5.30 Measuring locations of battery surface temperature (testing vehicle B)

Figure 5.31 Measuring location of battery cooling air temperature (testing vehicle B)

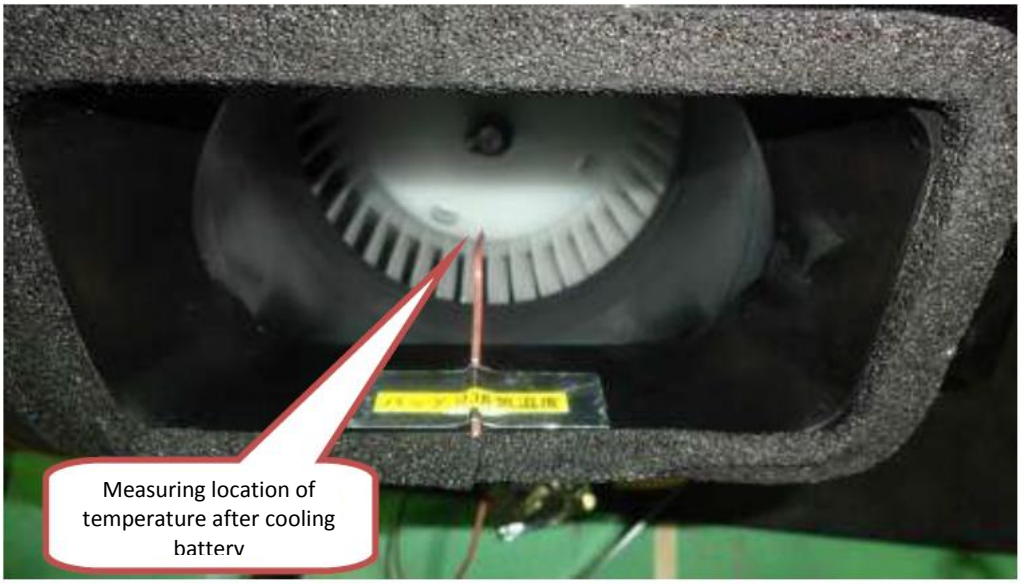

Figure 5.32 Measuring location of temperature after cooling battery (testing vehicle B)

Figure 5.32 Measuring location of wheel driving power (testing vehicle B)

5.2.4 Measured items and measuring locations of testing vehicle C

Table 5.7 shows items measured, their measuring locations, measuring methods and devises used for measurement (manufacturers of the devices, model number, etc.) regarding testing vehicle C. Figure 5.34 shows measuring devices installed in the interior of the vehicle.

To determine the operating conditions of the engine, the rotational speed and the load are required. For the engine rotational speed, the rotational speed of the crank pulley was measured. For the engine load, while the torque cannot be directly measured, measurements such as the throttle opening rate, the intake pipe pressure and the fuel flow rate can be used as replacements. Because the throttle of the testing vehicle is electronically controlled, its opening rate could not be measured from outside. The intake pipe pressure was measured by splitting the genuine piping. To measure the fuel flow rate, as shown in Figure 5.35, the genuine pipe was extended and a flowmeter was inserted in the fuel line. In addition, to verify the replicability of the test, the engine water temperature, the engine oil temperature and the temperature of the air surrounding the engine were measured. The engine water temperature was measured by inserting a pipe in the genuine engine cooling water hose. The engine oil temperature was measured with a thermocouple affixed to the oil level gauge.

To determine operating conditions of the motor, measurements such as the motor rotational speed and the torque are necessary, but they cannot be directly measured because the motor is installed inside the transmission. For this reason, as shown in Figure 5.36, the AC voltage and the electronic current, which are input to the front motor, were measured on the front inverter. Also, because the front motor is cooled with the oil cooling system that uses the ATF, the oil drain plug was modified and the ATF temperature was measured. With regard to the rear motor, as shown in Figure 5.37, the AC voltage and the electronic current were measured on the rear inverter. Because the rear motor is cooled with water, the cooling water temperature was measured.

With regard to the battery, the service plug was modified and the DC electronic current was measured. Since the voltage is the same as the input voltage of the inverter, it was skipped with the battery. The

battery surface temperature was measured, as shown in Figure 5.38, at three locations. The temperature of the battery cooling air was also measured.

As the vehicle's driving power, the wheel driving power was measured. As shown in Figure 5.39, a six-component force meter was installed on front and rear driving wheels. To measure the vehicle's acceleration, an accelerometer was installed near the centre of the vehicle's body.

Table 5.7 Measurements taken of the testing vehicle C

Item	Name	Location	Method	Name of devise used for measurement
Engine	Engine rotational speed	Crank pulley	Optical sensor	Keyence FS-V21
	Throttle opening rate	Measurement not possible		
	Intake pipe pressure	Vacuum hose	Vacuum gauge	Keyence AP-44
	Fuel flow rate	Entrance of engine	Fuel flowmeter	Ono Sokki FP-213S
	Fuel temperature	Entrance of engine	Sheathed thermocouple	Type T
	Water temperature	Exit of engine	Sheathed thermocouple	Type T
	Intake air temperature	Air cleaner	Thermocouple	Type T
	Oil temperature	Level gauge	Sheathed thermocouple	Type T
	Air temperature around engine	Above engine	Thermocouple	Type T
Front motor	Motor rotational speed	Measurement not possible		
	Motor input voltage (AC)	Top of inverter	Wattmeter	Hioki E.E. Corp. 3194
	Motor input electric current (AC)	Top of inverter	Clamp meter	Hioki E.E. Corp. 9277 x 3
	ATF temperature	Transmission drain	Sheathed thermocouple	Type T
Front inverter	Inverter voltage (DC)	Top of inverter	Wattmeter	Hioki E.E. Corp. 3390
	Inverter electric current (DC)	Top of inverter	Wattmeter	Hioki E.E. Corp. 9278
	Inverter temperature	Exit of inverter cooling water	Sheathed thermocouple	Type T
Rear motor	Motor rotational speed	Measurement not possible		
	Motor input voltage (AC)	Top of inverter	Wattmeter	Hioki E.E. Corp. 3194
	Motor input electric current (AC)	Top of inverter	Clamp meter	Hioki E.E. Corp. 9277 x 3
	Motor temperature	Exit of motor cooling water	Sheathed thermocouple	Type T
Rear inverter	Inverter electric current (DC)	Top of inverter	Wattmeter	Hioki E.E. Corp. 9278
Battery	Battery electronic current	Service plug	Clamp meter	Hioki E.E. Corp. 9278
	Battery surface temperature	Surface of battery	Thermocouple	Type T x 3

	Battery cooling air temperature	Exit port of cooling air	Thermocouple	Type T
Vehicle	Wheel driving power on front right	Wheel	Six-component force meter	Kyowa Electronic Instruments WFT-B-8KNSB13
	Wheel driving power on rear right	Wheel	Six-component force meter	
	Roller driving power	Chassis dynamometer	Load cell	–
	Wheel rotational speed on left	Wheel	Six-component force meter	Kyowa Electronic Instruments WFT-B-8KNSB13
	Wheel rotational speed on right	Wheel	Six-component force meter	
	Vehicle speed	Interior (on-road test)	GPS vehicle speedometer	Vios System VGVS-SP5Ci
		Chassis dynamometer (chassis dynamometer test)	Chassis dynamometer	Meidensha
	Vehicle acceleration	Interior	Accelerometer	Kyowa Electronic Instruments AS-1TG

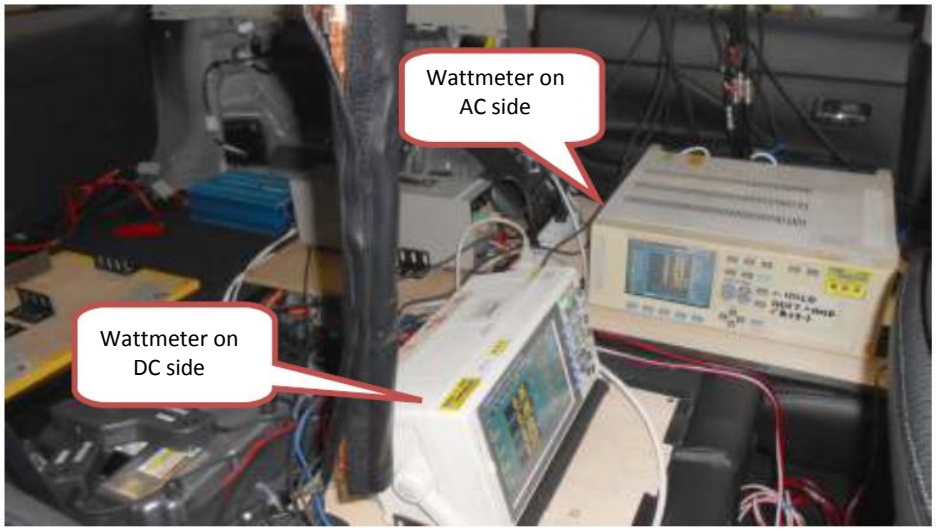

Figure 5.34 Measuring devices in the interior (testing vehicle C)

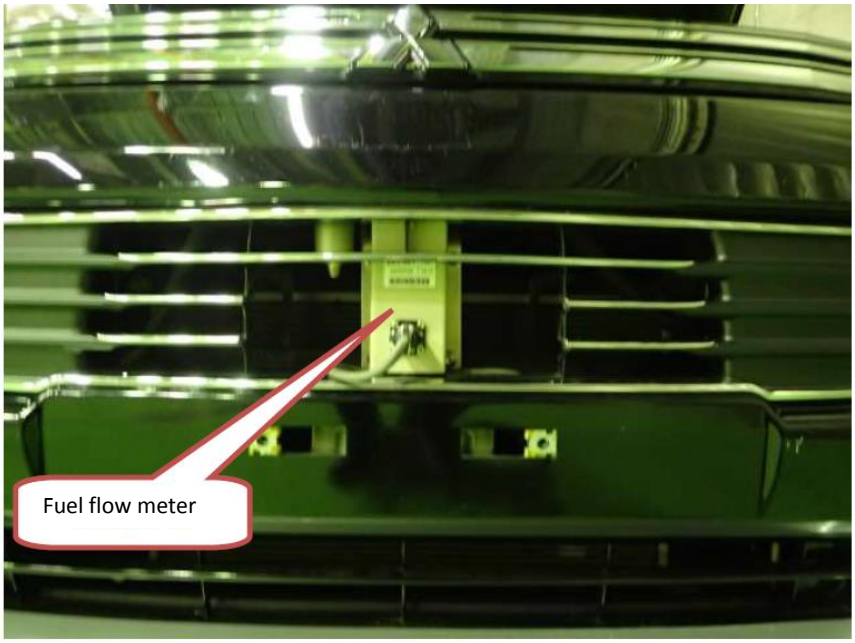

Figure 5.35 Measuring location of fuel flow rate (testing vehicle C)

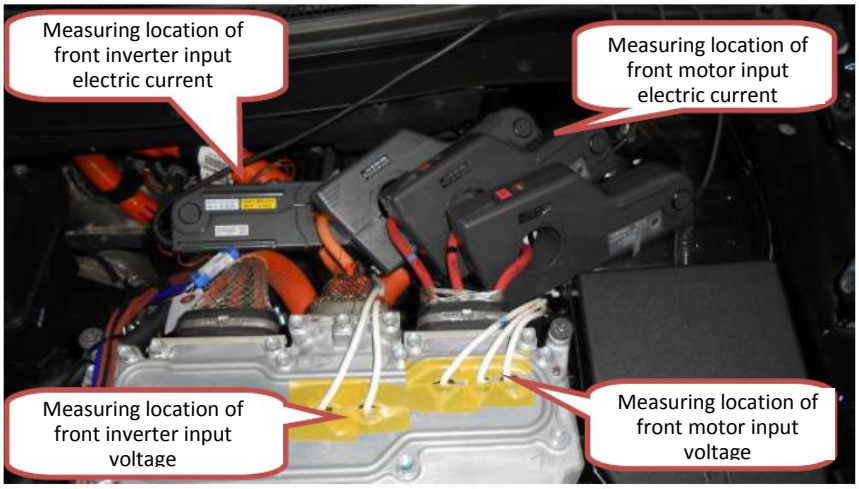

Figure 5.36 Measuring locations of front motor and inverter (testing vehicle C)

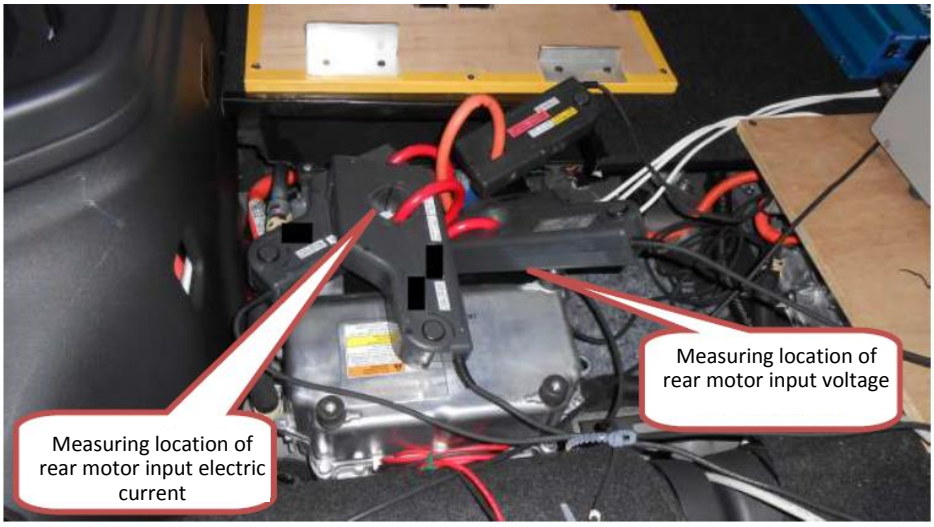

Figure 5.37 Measuring locations of rear motor and inverter (testing vehicle C)

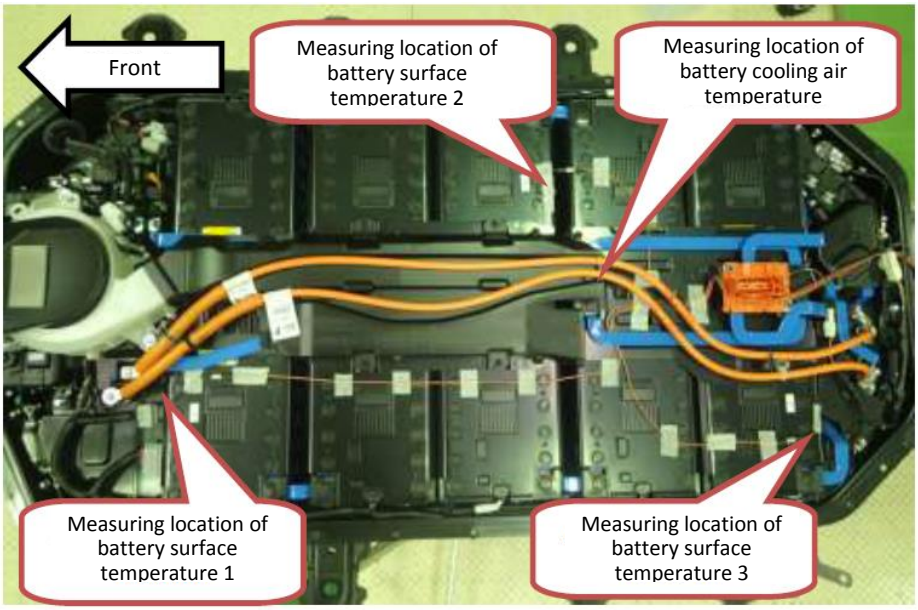

Figure 5.38 Measuring locations of battery surface temperature (testing vehicle C)

Figure 5.39 Measuring location of wheel driving power output (testing vehicle C)

5.2.5 Measurements necessary to calculate operating conditions at the time of the maximum power output of HEV systems

Measurements necessary to calculate the engine power output are the engine rotational speed and the torque, but since the engine torque is difficult to measure from outside, the engine power output cannot be directly determined. For this reason, in the method proposed to the ISO, the engine rotational speed and the maximum power output curve are measured in a test of the engine on its own conducted in advance, and the power output that corresponds to the engine rotational speed at the time of the HEV system's maximum power output is deemed as the engine power output at the time of the HEV system's maximum power output. In this method, the throttle conditions need to be equal between the time of maximum power generation in the engine unit test and the time when the HEV system power output is measured, and to verify this, the throttle opening that is necessary to calculate operating conditions in the direction of the engine load needs to be measured and the opening has to be the same as that in the engine unit test. As shown in Table 5.8, the throttle opening could not be directly measured with any of the three testing vehicles in this study. Therefore, something that can be used as a replacement for the throttle opening needs to be measured. For that purpose, the intake pipe pressure and fuel flow rate can be used. In the present study, it was confirmed that the intake pipe pressure, which can be relatively easily measured when the HEV system power output is measured, is the same as that in the engine unit test. Results with testing vehicle A are shown in Figure 5.40. The x-axis represents time, the left y-axis represents intake pipe pressure, and the right y-axis represents HEV system power output. In terms of testing conditions, the vehicle speed was 160 km/h, warming up was done at the constant speed of 60 km/h for 20 minutes and the SOC at the start of the test was 80%. The facility used for the test was the chassis dynamometer. The HEV system power output became maximum around 13 seconds and the intake pipe pressure then was found to be almost identical to the intake pipe pressure in the engine unit test. This confirmed that if the intake pipe pressure is measured, it can be used as a replacement for the throttle opening.

Measurements necessary to calculate the motor power output are the motor rotational speed and the torque, but because the motor itself is installed within the transmission case, neither the motor rotational speed nor the torque can be measured directly from outside, and therefore the mechanical power output cannot be directly determined. For this reason, it was decided that the motor input voltage and electric current, which can be measured from outside, should be measured, although what the result would show was electric power. Because all the three testing vehicles of the present study had the motor and the inverter connected with cables, the electric current could be measured. Also, because the cables were connected to terminal blocks, it was found that the voltage could be measured relatively easily. Therefore, the motor input electric power could be measured.

Measurements necessary to calculate the battery power are the battery voltage and electric current, and they could be measured relatively easily with the three testing vehicles of this study, though locations where measurements could be taken easily were different with each vehicle.

Based on the above results, it was understood that operating conditions of the engine and the battery at the time of the maximum HEV system power output could be determined. With regard to the motor, the shaft output could not be directly measured, and measurements necessary to calculate operating conditions, such as the motor rotational speed, are also difficult to obtain. The motor input electric power could be measured with the testing vehicles of this study, but with vehicles in which the connections between the inverter and the motor are made in the transmission case, the measurement could be difficult.

Table 5.8 Measurements necessary to determine operating conditions and their measurability

Testing vehicle	A	B	C
Engine rotational speed	✓	✓	✓
Throttle opening	N	N	N
Intake pipe pressure	✓	✓	✓
Fuel flow rate	✓	✓	✓
Motor rotational speed	N	N	N
Motor torque	N	N	N
Motor input voltage (AC)	✓	✓	✓
Motor input electric current (AC)	✓	✓	M
Battery voltage (DC)	✓	✓	✓
Battery electric current (DC)	✓	✓	✓

✓: measurable M: requires a partial modification

N: measurement not possible (would require help from the manufacturer of the vehicle)

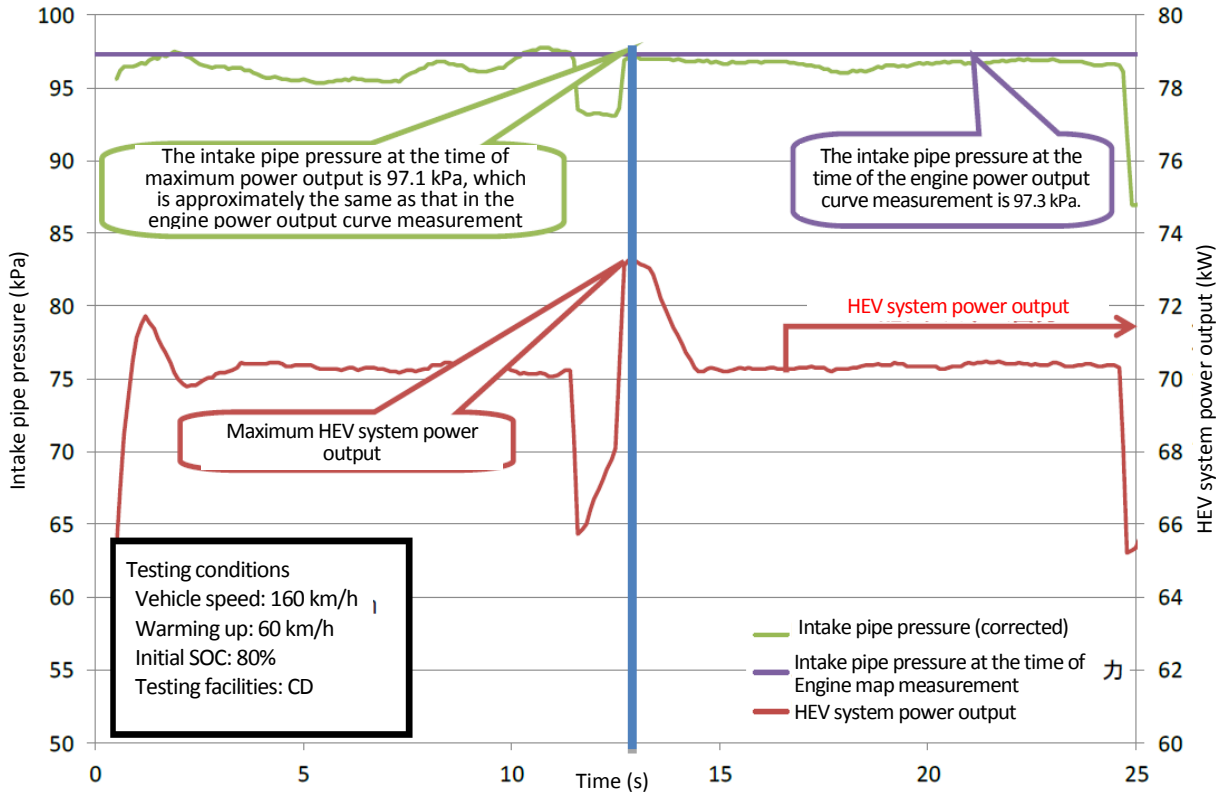

Figure 5.40 Intake pipe pressure and HEV system power output of testing vehicle A

5.2.6 Summary

Whether or not measurements that are necessary to determine operating conditions of the engine, motor and battery at the time of maximum power output of the HEV system can be taken the same way on differently-structured HEV systems without significantly modifying the vehicles was examined. Where some measurements could not be taken, whether operating conditions could be determined only on measurements that could be obtained was studied. Where operating conditions could be determined, the differences between the calculated HEV system power based on those measurements and the manufacturers' listed power values were reviewed.

The results showed that with regard to the engine operating conditions, by measuring the engine rotational speed and the intake pipe pressure, the engine power output could be calculated. With regard to the motor, neither the motor rotational speed nor the motor torque could be measured and only the input voltage and electronic current could be measured. The motor operating conditions could not be determined based on these measurements. With regard to the battery, both the voltage and the electronic current could be measured.

Following protocols of the method proposed to the ISO, tests were conducted with the chassis dynamometer. Table 5.9 shows the results of processing measured data through obtaining one-second moving averages. The engine power output was calculated based on the engine rotational speed and the power output curve were provided by the manufacturers' of the testing vehicles. As a result, testing vehicle A measured 73.1 kW at the vehicle speed of 160 km/h, which was 100% of the manufacturer's listed value. Testing vehicle B measured 95.3 kW at the vehicle speed of 115 km/h in the fourth gear, which was 94% of the listed value. Testing vehicle C measured 147.3 kW at the vehicle speed of 160

km/h, but because the manufacturer does not publicise the system power, the replicability of the measurement is unknown.

Table 5.9 Power output calculated by the method proposed to the ISO

Testing vehicle	A	B	C
Measurement of engine operating conditions	Engine rotational speed, intake pipe pressure	Engine rotational speed, intake pipe pressure	Engine rotational speed, intake pipe pressure
Measurement of battery operating conditions	Battery voltage, Battery electric current	Battery voltage, Battery electric current	Battery voltage, Battery electric current
HEV system power output	73.2 kW @160 km/h	95.3 kW @115 km/h	117.3 kW @160 km/h
Replicability compared to the manufacturer's listed values	100%	94%	System power not published

5.3 Study of effects that different types of testing conditions have on power output measurements of HEV

5.3.1 Effects of warm-up method

(1) Testing vehicle A

In order to study effects that different warm-up methods have on power output measurements of HEV, three types of warm-up methods were examined. First, as the cold condition, the engine, transmission and battery were soaked over 12 hours in the environment of 25 ^{o}C. As the second method, the vehicle was warmed up at the constant speed of 60 km/h for 20 minutes. Under this condition, because the warming-up is done at a constant speed, the engine and driveline are warmed up, but the battery is not much charged or drained and therefore the warm-up effect on the battery was expected to be small. As the third condition, the vehicle was warmed up through running it once in the JC08 mode. Under this condition, because the vehicle speed goes up and down, the battery was expected to be warmed up through charging and draining.

Figure 5.41 shows changes in temperature when the vehicle was operated for 20 minutes at the constant speed of 60 km/h after starting from the cold state. The x-axis represents time, the left y-axis represents temperature and the right y-axis represents vehicle speed. The facility used for the test is the chassis dynamometer. Results show that the engine water temperature reached approximately 85 ^{o}C after 600 seconds and then remained stable at the level. The engine oil temperature reached 80 ^{o}C after 1200 seconds. The ATF temperature was still going up at the 20th minute mark. On the other hand, it was observed that the inverter temperature and battery temperature were mostly unchanged.

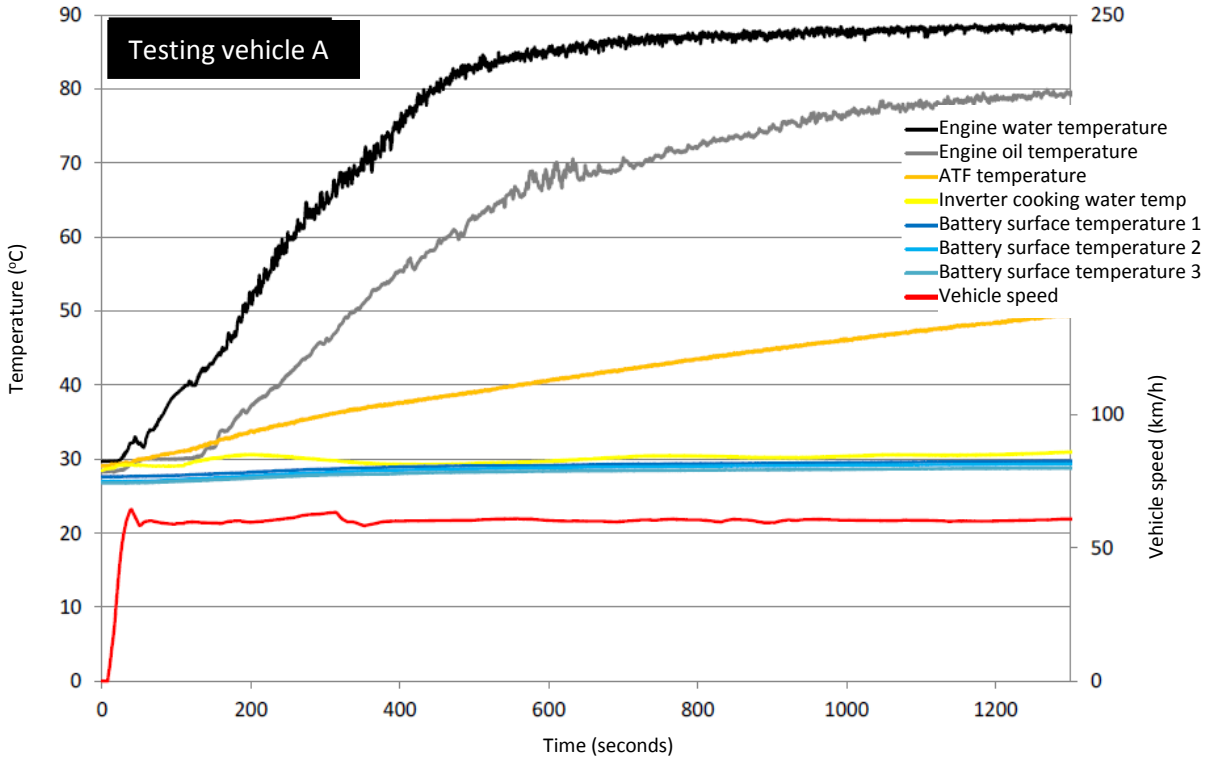

Figure 5.41 Changes in temperature when the vehicle was warmed up at the constant speed of 60 km/h (testing vehicle A)

Next, Figure 5.42 shows changes in temperature when the vehicle was warmed up in the JC08 mode starting from the cold state. The x-axis represents time, the left y-axis represents temperature and the right y-axis represents vehicle speed. The facility used for the test is the chassis dynamometer. Results show that the engine water temperature was approximately 60 °C after 600 seconds, revealing that after the operation in the mode, it did not reach 80 °C. The engine oil temperature showed the same trend as the engine water temperature and was around 55 °C after 1200 seconds. The ATF temperature was around 40 °C after the JC08 mode operation and was still in the process of going up. The inverter temperature and battery temperature showed a slight upward trend.

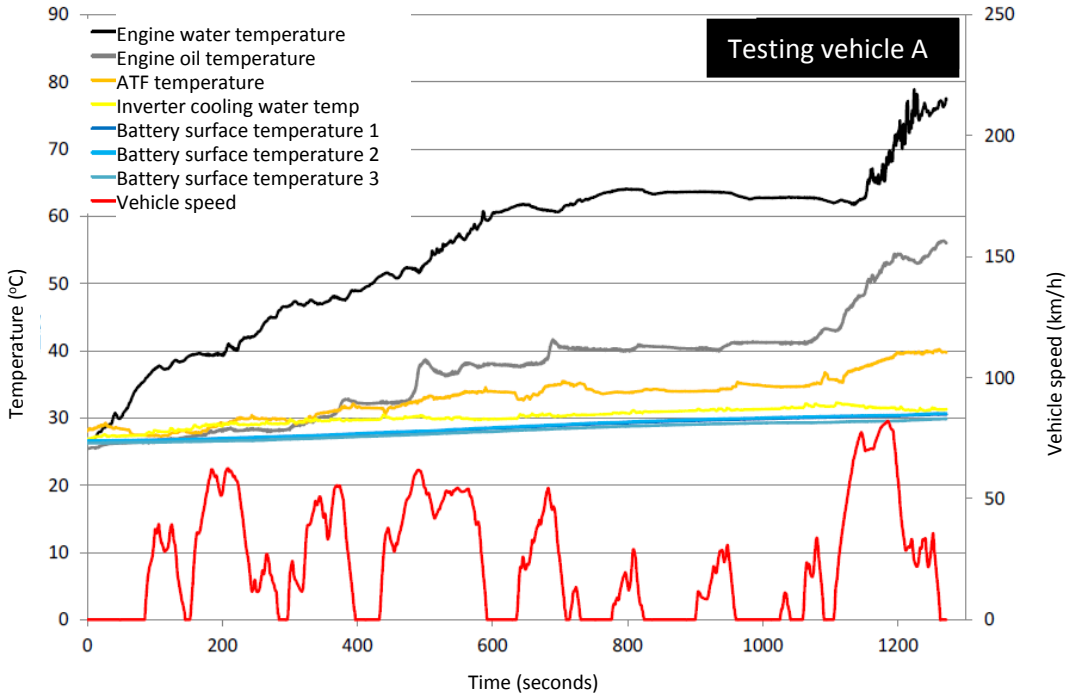

Figure 5.42 Changes in temperature when the vehicle was warmed up through JC08 mode operation (testing vehicle A)

Table 5.10 shows differences in temperature before and after the warm-up operations starting from the cold state of 25 °C were completed, as calculated from the above results. The engine water temperature increased by 63.6 °C when the vehicle was warmed up at the constant speed of 60 km/h, and by 52.1 °C when the vehicle was warmed up through the JC08 mode. The warming up at the constant speed of 60 km/h resulted in a temperature increase 12.5 °C larger than that through the JC08 mode. Similarly, the warming up at the constant speed of 60 km/h resulted larger temperature increases, in the engine oil temperature by 23.3 °C and in the ATF temperature by 9.6 °C. It was understood that the engine and the driveline, such as the automatic transmission, warmed up faster through the 60 km/h constant speed warm-up because the engine was operating throughout. The inverter temperature went up around 6 °C when the vehicle was warmed up at the constant speed of 60 km/h and through the JC08 mode operation; the difference in the warm-up method had little effect. With regard to the battery temperature, when the vehicle was warmed up at the constant speed of 60 km/h, the temperature measured at three locations went up, on average, 4.5 °C, and the JC08 mode warm-up resulted in 5.4 °C increase; as expected, the JC08 mode warm-up resulted in a larger temperature increase, by 0.9 °C.

Table 5.10 Differences in temperature before and after warming-up by different methods (testing vehicle A)

Warm-up conditions	Engine water temp.	Engine oil temp.	ATF temp.	Inverter cooling water temp.	Battery surface temp. 1	Battery surface temp. 2	Battery surface temp. 3
60 km/h	63.6 °C	54.7 °C	24.5 °C	6.1 °C	4.9 °C	4.5 °C	4.0 °C
JC08	52.1 °C	31.4 °C	14.9 °C	6.3 °C	5.6 °C	5.8 °C	4.9 °C

Next, Figure 5.43 shows effects of differences in temperature increase due to different warm-up methods on power output measurements. In terms of testing conditions, the vehicle speed was 160 km/h and the initial SOC was 80%. The axle-hub chassis dynamometer was used as the texting facility. To compare warm-up methods, the case where the vehicle was warmed up at the constant speed of 60 km/h was used as the standard and the cold condition and the JC08 mode warm-up were compared against it. Under the cold condition, because the vehicle was started from the cold state and measurements were taken after the vehicle was accelerated with the dynamometer to the testing speed, which took several tens of seconds, the engine water temperature, etc. were slightly increased. For testing the warm-method of 20 minutes at a constant speed of 60 km/h and the warm-up method in the JC08 mode, the warm-up did not start with the vehicle being in the completely cold state but it was started after the battery temperature was forcibly lowered to 25 ^{o}C after the preceding test, and therefore the warm-up started with engines, etc. somewhat warmer already. The power outputs were compared in the wheel driving power, of which affecting factors included warm-up of the transmission, and in the total of the engine power output and the battery power, which is being proposed to the ISO.

In wheel driving power output, compared with the average value of 63.0 kW with the 60 km/h constant speed warm-up, that of the cold condition was 3.6 kW lower and the JC08 mode warm-up resulted in a value 1.2 kW higher. This showed that average values of power output were different by more than 1.0 kW, indicating that warm-up methods meaningfully affect power output measurements. Deviations were -1.5 to 1.0 kW with the 60 km/h constant speed warm-up, -2.3 to 1.0 kW under the cold condition, and -1.7 to 1.4 kW in the JC08 mode; measurements varied widely under the cold conditions.

When the power output was calculated by the method proposed to the ISO, which is to add the engine power output and the battery power, compared with the average value of 72.6 kW with the 60 km/h constant speed warm-up, that of the cold condition was 0.3 kW lower and the JC08 mode warm-up resulted in a value 0.4 kW higher. This showed that average values of power output were different by 1.0 kW or less, indicating that warm-up methods' effects on power output measurements were small. Deviations were ±0.2 kW with the 60 km/h constant speed warm-up, -1.0 to 0.5 kW under the cold condition, and ±0.1 kW in the JC08 mode; measurements varied widely under the cold conditions.

Further, power output measurements were compared between the two measuring locations: the method proposed to the ISO, which is to add the engine power output and the battery power to obtain upper-most stream measurements, and the wheel driving power output, which includes power loss in the transmission. In the wheel driving power output, obtained values were 12.9 kW lower under the cold condition, 9.6 kW lower with the 60 km/h constant speed warm-up, and 8.8 kW lower the JC08 mode warm-up. This revealed that in the calculation method proposed to the ISO, no warm-up method produced a widely different power output value, but in wheel driving power output measurements, differences in warm-up methods resulted in differences in the warmed-up condition of the transmission and therefore affected power output measurements.

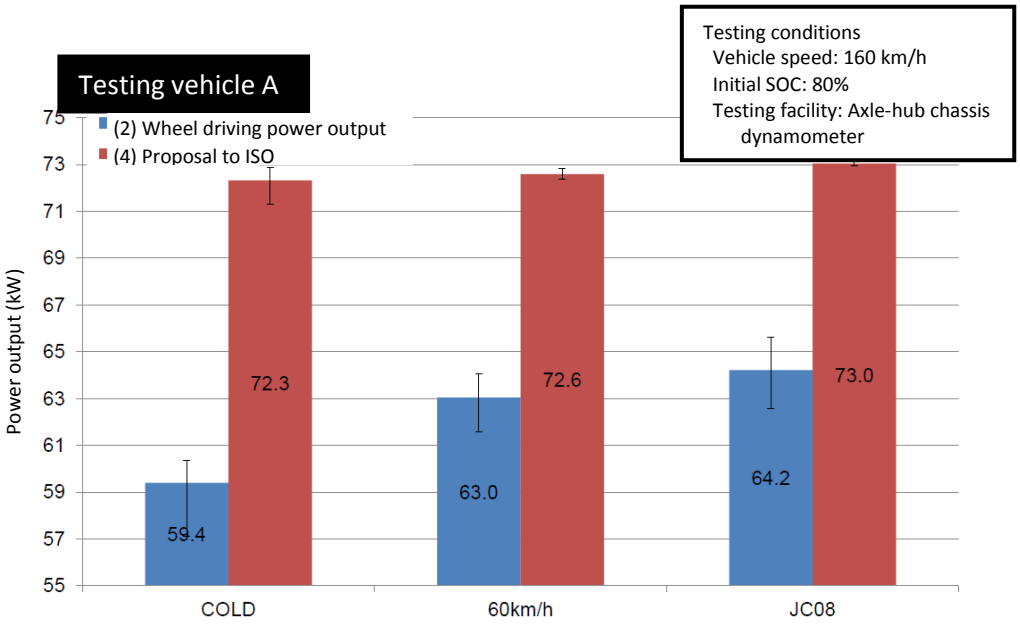

Figure 5.43 Effects of differences in temperature increase through different warm-up methods on power output measurements (testing vehicle A)

Figure 5.44 shows temperature at different locations at the time of maximum power output generation. The engine water temperature was the highest when the vehicle was warmed up at 60 km/h and 74.7 °C on average. Under the cold condition, it was 50.3 °C on average, 24.4 °C lower. When the warm-up was done in the JC08 mode, it was 72.1 °C on average and 2.6 °C lower than that of the 60 km/h warm-up. The engine oil temperature showed the same tendencies, with the 60 km/h warm-up resulted in the highest temperature, 74.3 °C on average, and the cold condition resulted in 42.9 °C on average, 31.4 °C lower. When the warm-up was done in the JC08 mode, it was 69.7 °C on average and 4.6 °C lower than that of the 60 km/h warm-up. With regard to the temperature related to the engine, when the vehicle was tested under the cold condition, because the length of time before the measurement could start varied, temperature measurements tended to be widely varied relative to the average value. The ATF temperature was the highest when the vehicle was warmed up in the JC08 mode, 65.3 °C on average and 0.9 °C higher compared with the temperature in the case of 60 km/h warm-up. Under the cold condition, it was 38.1 °C on average, which was 26.3 °C lower. The inverter cooling water temperature was the highest under the cold condition, at 31.9 °C on average, and 2.3 °C higher compared with that of the 60 km/h warm-up. When the vehicle was warmed up in the JC08 mode, the average inverter cooling water temperature was 29.7 °C, which was 0.1 °C higher than that of the 60 km/h warm-up. The battery temperature was the highest when the vehicle was warmed up in the JC08 mode and the average of measurements taken at three locations was 31.7 °C, which was 3.8 °C higher than 27.9 °C of the 60 km/h warm-up. It was 28.5 °C under the cold condition, which was 0.6 °C higher than that of the 60 km/h warm-up.

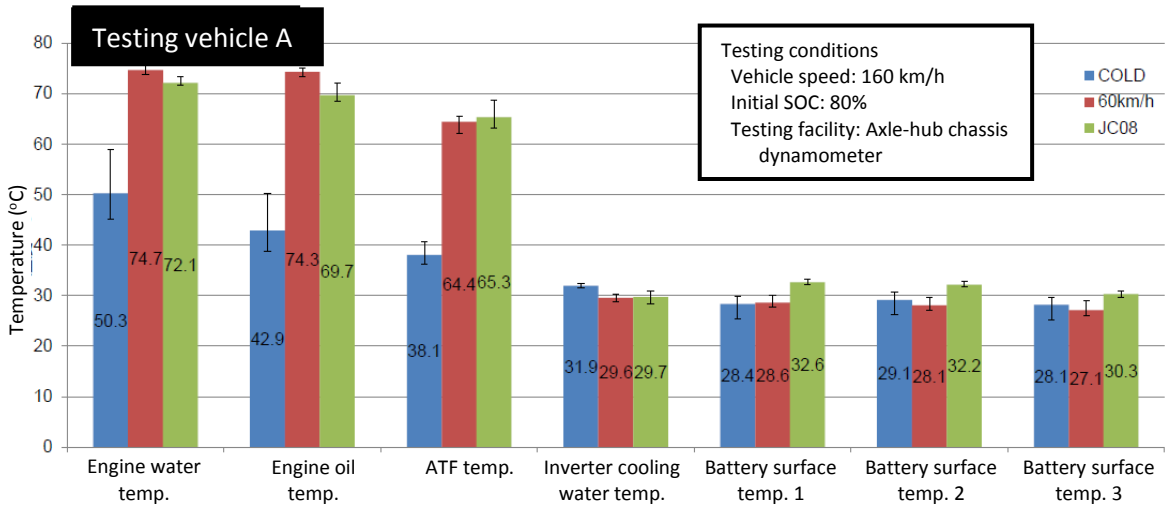

Figure 5.44 Temperature of different locations at the time of maximum power output generation (testing vehicle A)

(2) Testing vehicle B

Figure 5.45 shows changes in temperature when the vehicle was operated for 20 minutes at the constant speed of 60 km/h after starting from the cold state. The chassis dynamometer was used as the testing facility. Results show that the engine water temperature reached around 80 °C after approximately 300 seconds and then remained stable at the level. The engine oil temperature reached 80 °C after 1200 seconds. The ATF temperature was still going up at the 20th minute mark. It was observed that the inverter temperature and battery temperature showed slight upward trends. It is believed that this was due to the fact that, while operation at the constant speed of 60 km/h was not expected to cause the battery to charge or drain, because testing vehicle B repeats EV operations and HEV operations, even while running at the constant speed, the battery was frequently charged and drained.

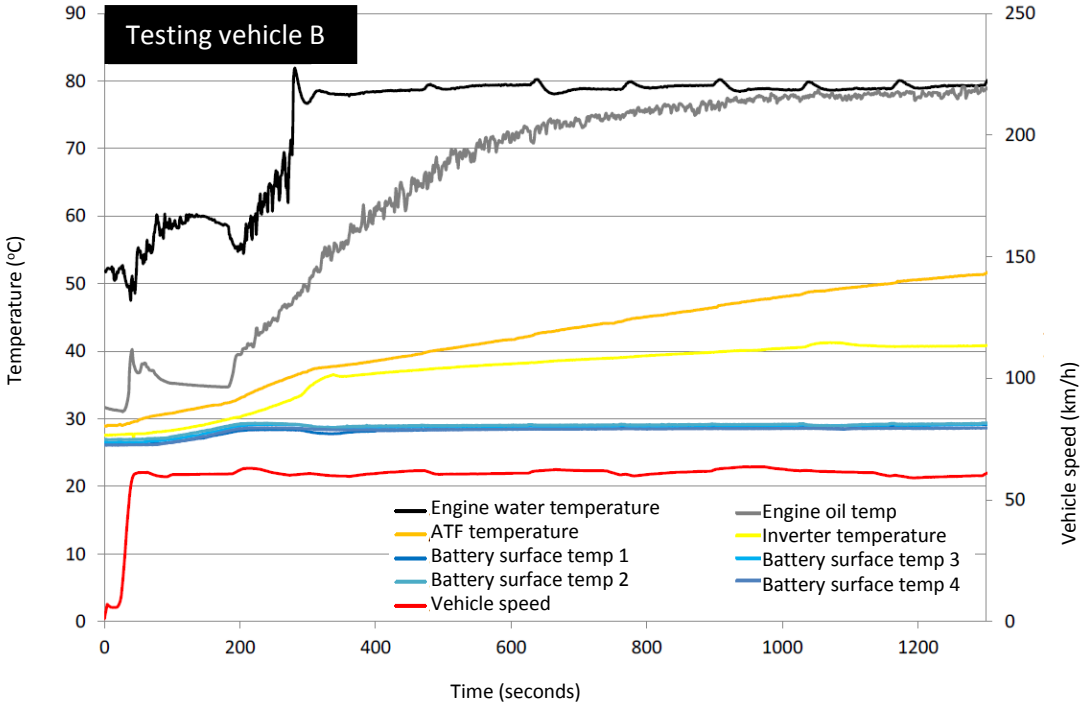

Figure 5.45 Changes in temperature when the vehicle was warmed up at the constant speed of 60 km/h (testing vehicle B)

Next, Figure 5.46 shows changes in temperature when the vehicle was running in the JC08 mode starting from the cold state. Results show that the engine water temperature was approximately 80 °C after approximately 500 seconds, and then remained steady. The engine oil temperature showed the same trend as the engine water temperature and was around 75 °C after approximately 1200 seconds. The ATF temperature was around 40 °C after the JC08 mode operation and was still in the process of going up. The inverter temperature and battery temperature showed slight upward trends.

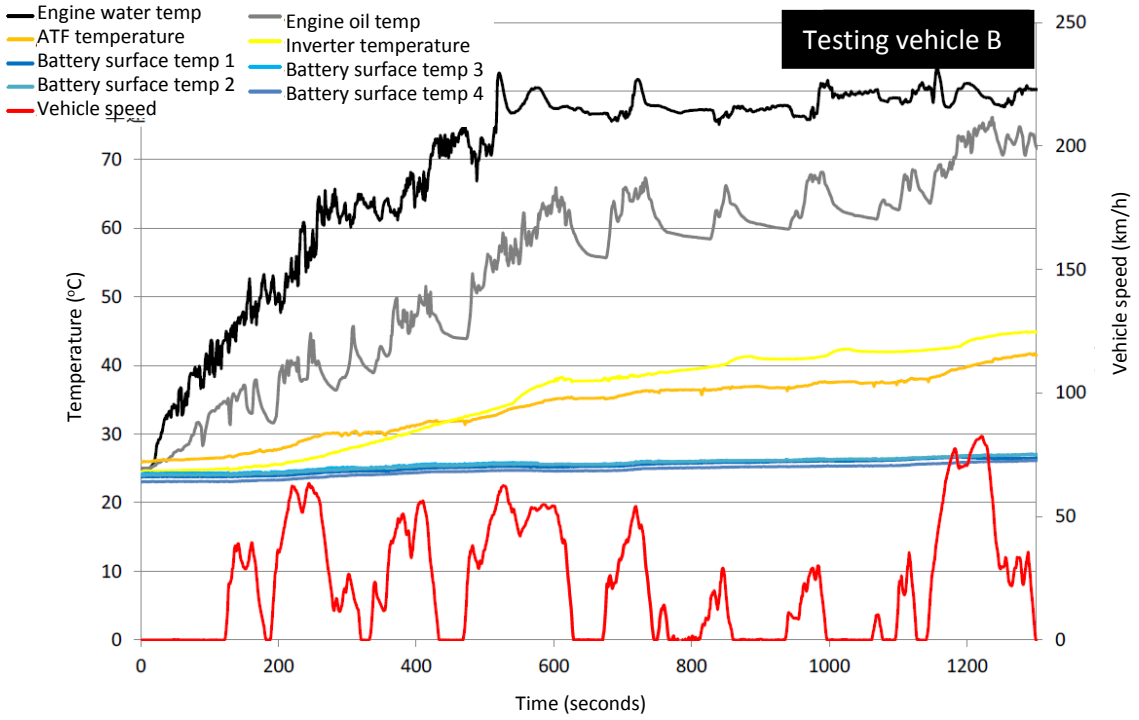

Figure 5.46 Changes in temperature when the vehicle was warmed up through JC08 mode operation (testing vehicle B)

Table 5.11 shows differences in temperature before and after the warm-up operations starting from the cold state of 25 °C were completed. The engine water temperature increased by 54.3 °C when the vehicle was warmed up at the constant speed of 60 km/h, and by 53.0 °C when the vehicle was warmed up through the JC08 mode. The warming up at the constant speed of 60 km/h resulted in a temperature increase 1.3 °C larger than that through the JC08 mode. Similarly, the warming up at the constant speed of 60 km/h resulted larger temperature increases, in the engine oil temperature by 6.3 °C and in the ATF temperature by 10 °C. It was understood that the engine and the driveline, such as the automatic transmission, warmed up faster through the 60 km/h constant speed warm-up. The inverter temperature went up around 13.2 °C when the vehicle was warmed up at the constant speed of 60 km/h and 20.2 °C through the JC08 mode operation; the JC08 mode warm-up resulted in a temperature increase 7.0 °C larger than the 60 km/h warm-up. With regard to the battery temperature, when the vehicle was warmed up at the constant speed of 60 km/h, the temperature measured at four locations went up, on average, 2.6 °C, and the JC08 mode warm-up resulted in 2.8 °C increase; the difference in the warm-up methods had little effect.

Table 5.11 Differences in temperature before and after warming-up by different methods (testing vehicle B)

Warm-up conditions	Engine water temp.	Engine oil temp.	ATF temp.	Inverter cooling water temp.	Battery surface temp. 1	Battery surface temp. 2	Battery surface temp. 3	Battery surface temp. 4
60 km/h	54.3 °C	54.0 °C	26.2 °C	13.2 °C	3.0 °C	2.6 °C	2.3 °C	2.5 °C
JC08	53.0 °C	47.7 °C	16.2 °C	20.2 °C	2.7 °C	2.7 °C	2.9 °C	3.0 °C

Next, Figure 5.47 shows effects of differences in temperature increase due to different warm-up methods on power output measurements. In terms of testing conditions, the vehicle speed was 68 km/h in the third gear and the initial SOC was 93%. The axle-hub chassis dynamometer was used as the texting facility. To compare warm-up methods, the case where the vehicle was warmed up at the constant speed of 60 km/h was used as the standard and the cold condition and the JC08 mode warm-up were compared against it. The power outputs were compared in the wheel driving power, of which affecting factors included warm-up of the transmission, and in the total of the engine power output and the battery power, which is being proposed to the ISO.

In wheel driving power output, compared with the average value of 84.8 kW with the 60 km/h constant speed warm-up, that of the cold condition was 1.5 kW lower and the JC08 mode warm-up resulted in a value 1.2 kW lower. This showed that average values of power output were different by more than 1.0 kW, indicating that warm-up methods meaningfully affect power output measurements. Deviations were -1.9 to 1.7 kW with the 60 km/h constant speed warm-up, -1.3 to 1.2 kW under the cold condition, and -0.6 to 0.4 kW in the JC08 mode; measurements varied widely with the 60 km/h constant speed warm-up.

When the power output was calculated by the method proposed to the ISO, which is to add the engine power output and the battery power, compared with the average value of 92.6 kW with the 60 km/h constant speed warm-up, that of the cold condition was 1.4 kW higher and the JC08 mode warm-up resulted in a value 1.0 kW higher. This showed that average values of power output were different by more than 1.0 kW, indicating that warm-up methods somewhat affect power output measurements. Deviations were -0.3 to 0.4 kW with the 60 km/h constant speed warm-up, which means stable measurement, ±1.0 kW under the cold conditions, and -1.1 to 0.5 kW in the JC08 mode; measurements varied somewhat widely.

Further, power output measurements were compared between the two measuring locations: the method proposed to the ISO, which is to add the engine power output and the battery power to obtain upper-most stream measurements, and the wheel driving power output, which includes power loss in the transmission. In the wheel driving power output, obtained values were 10.7 kW lower under the cold conditions, 7.8 kW lower with the 60 km/h constant speed warm-up, and 10 kW lower the JC08 mode warm-up. This revealed that in the calculation method proposed to the ISO, no warm-up method produced a widely different power output value, but in wheel driving power output measurements, differences in warm-up methods resulted in differences in the warmed-up condition of the transmission and therefore affected power output measurements.

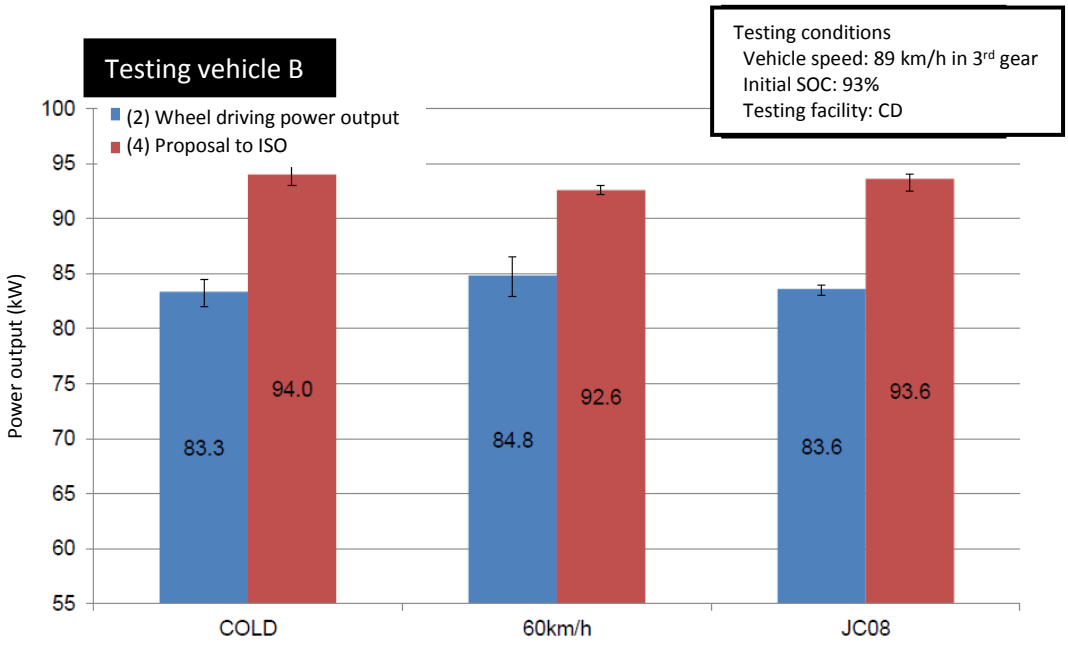

Figure 5.47 Effects of differences in temperature increase through different warm-up methods on power output measurements (testing vehicle B)

Figure 5.48 shows temperature at different locations at the time of maximum power output generation. The engine water temperature was 72.4 °C on average when the vehicle was warmed up at 60 km/h and under cold condition, it was 50.09°C on average, 21.5 °C lower. When the warm-up was done in the JC08 mode, it was 79.4°C on average and 7.0 °C higher than that of the 60 km/h warm-up. The engine oil temperature showed the same tendencies; with the 60 km/h warm-up it was 69.6°C on average, and the cold condition resulted in 39.9 °C on average, 29.7 °C lower. When the warm-up was done in the JC08 mode, it was 72.2 °C on average and 2.6 °C higher than that of the 60 km/h warm-up. With regard to the temperature related to the engine, because the vehicle repeats EV operations and HEV operations when it is warmed up at the constant speed of 60 km/h, the temperature changes greatly depending on in which mode it is operating when the warm-up is completed. For this reason, measurements tended to vary greatly compared with the average values. The ATF temperature was 62.1 °C on average when the vehicle was warmed up at 60 km/h, and under cold condition, it was 29.8 °C, 32.3 °C lower. With the JC08 mode warm-up, it was 57.2 °C on average and 4.9 °C higher compared with the temperature in the case of 60 km/h warm-up. The inverter temperature was 48.2 °C on average with the 60 km/h warm-up, and under cold condition, it was 26.9 °C on average, 21.3 °C lower. When the vehicle was warmed up in the JC08 mode, the average inverter temperature was 47.9 °C, which was about the same as that of the 60 km/h warm-up. With regard to the battery temperature, when the vehicle was warmed up in the JC08 mode, the average of measurements taken at four locations was 29.3 °C, and it was 31.1 °C with the 60 km/h warm-up, 1.8 °C higher. Under cold condition, it was 25.8 °C on average and 3.5 °C lower than the JC08 mode. The inverter cooling water temperature and battery surface temperature rose most when the vehicle was warmed up at 60 km/h.

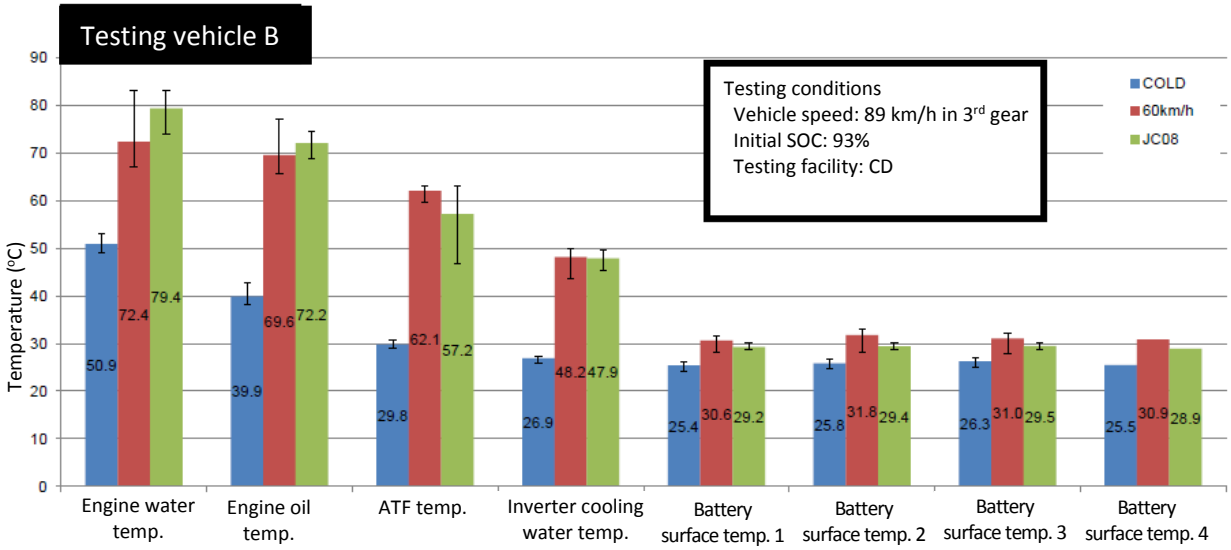

Figure 5.48 Temperature of different locations at the time of maximum power output generation (testing vehicle B)

(3) Testing vehicle C

Figure 5.49 shows changes in temperature when the vehicle was operated for 20 minutes at the constant speed of 60 km/h after starting from the cold state. The x-axis represents time, the left y-axis represents temperature and the right y-axis represents vehicle speed. The axle-hub chassis dynamometer was used as the testing facility. Results show that the engine water temperature reached around 80 °C after approximately 320 seconds and then remained stable at the level. The engine oil temperature reached 80 °C after approximately 1100 seconds. The ATF temperature was still going up at the 20th minute mark. It was observed that the inverter temperature and battery temperature showed slight upward trends.

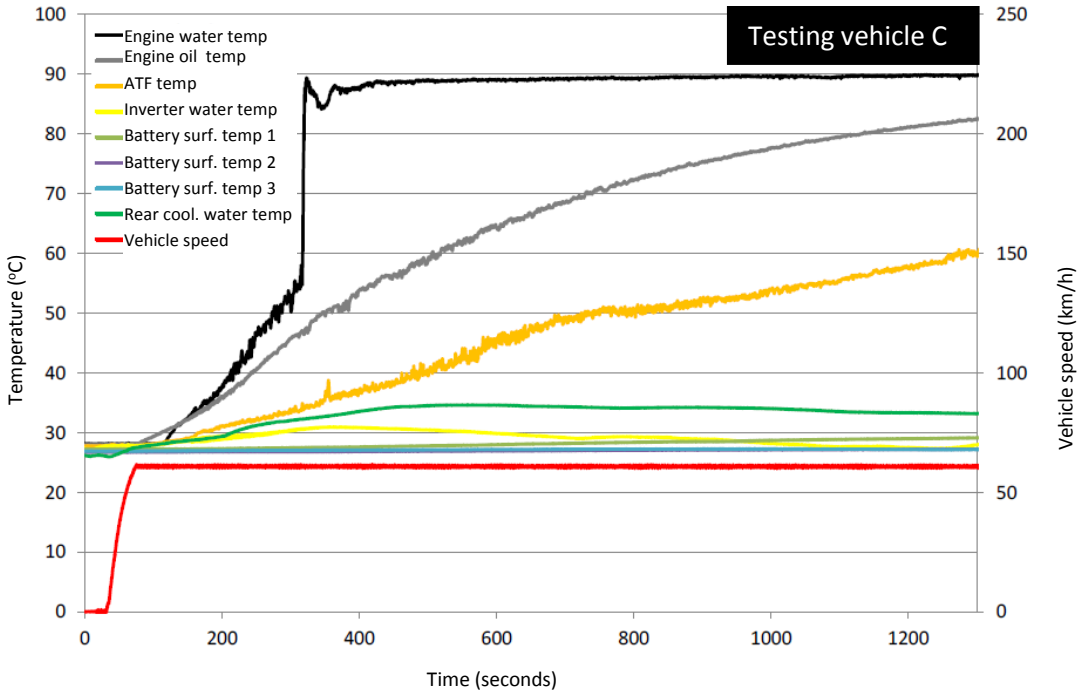

Figure 5.49 Changes in temperature when the vehicle was warmed up at the constant speed of 60 km/h (testing vehicle C)

Next, Figure 5.50 shows changes in temperature when the vehicle was running in the JC08 mode starting from the cold state. Results show that the engine water temperature was approximately 80 °C after approximately 500 seconds, and then remained steady. The engine oil temperature rose gradually and was around 70 °C after 1200 seconds. The ATF temperature was around 45 °C after the JC08 mode operation and was still in the process of going up. The inverter temperature and battery temperature showed slight upward trends.

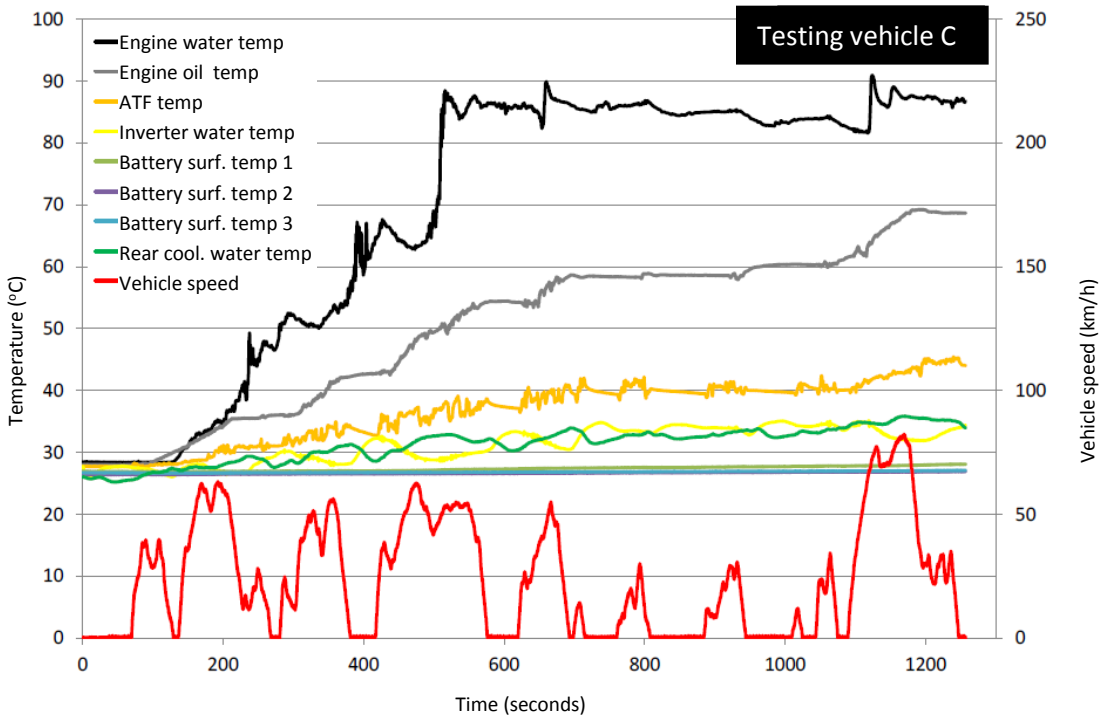

Figure 5.50 Changes in temperature when the vehicle was warmed up through JC08 mode operation (testing vehicle C)

Based on the opinion expressed in the Hybrid Group that testing with the WLTC mode, which is an international standard, would better facilitate discussions at ISO's international meetings than data obtained using the JC08 mode, which is Japan's domestic standard, the WLTC mode was added as a warm-up methods to be tested with testing vehicle C. Temperature changes during the WLTC mode operation starting from the cold condition are shown in Figure 5.51. Results show that the engine water temperature reached about 80 °C after approximately 450 seconds and after the 700th second mark, it remained stable around 87 °C . The engine oil temperature rose gradually and after the completion of *Extra High*, it was around 95 °C. The ATF temperature was approximately 65 °C after the completion of *Extra High* and was still going up. The inverter and battery temperatures were observed to show slight upward trends.

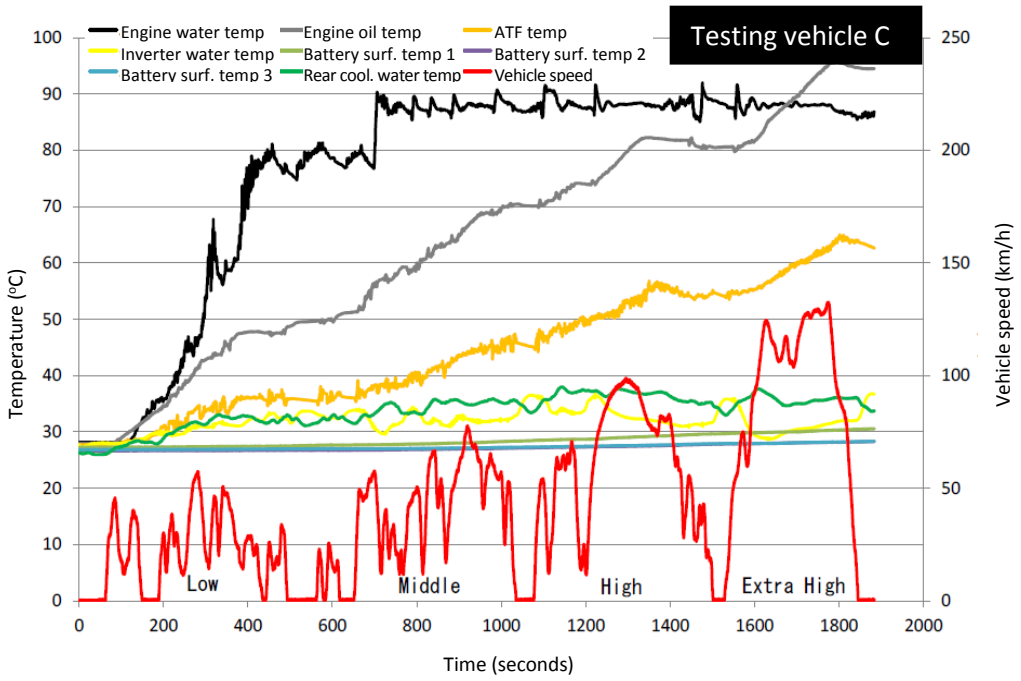

Figure 5.51 Changes in temperature when the vehicle was warmed up through WLTC mode operation (testing vehicle C)

Table 5.12 shows differences in temperature between the cold state of 25 °C and after the warm-up operations were completed. The engine water temperature increased by 61.5 °C when the vehicle was warmed up at the constant speed of 60 km/h, and by 58.3 °C when the vehicle was warmed up through the JC08 mode. The warming up at the constant speed of 60 km/h resulted in a temperature increase 3.2 °C larger than that through the JC08 mode, but since the temperature became steady after around the 500th second mark, the difference is not thought to be large. However, the engine oil temperature and the ATF temperature did not stabilize after the warming-up operations were complete and therefore warm-up methods have effects. The engine oil temperature increased 16.9 °C more with the 60 km/h warm-up than with the JC08 mode, and the ATF temperature increased 18.2 °C more with the 60 km/h warm-up. It was understood that the engine and the driveline, such as the automatic transmission, warmed up faster through the 60 km/h constant speed warm-up. The front inverter water temperature went up 5.4 °C when the vehicle was warmed up at the constant speed of 60 km/h and 6.7 °C through the JC08 mode operation; the JC08 mode warm-up resulted in a temperature increase 1.3 °C larger than the 60 km/h warm-up. The rear inverter water temperature went up 9.8 °C when the vehicle was warmed up at the constant speed of 60 km/h and 8.0 °C through the JC08 mode operation; the 60 km/h warm-up resulted in a temperature increase1.8 °C larger than the JC08 mode warm-up. With regard to the battery temperature, when the vehicle was warmed up at the constant speed of 60 km/h, the temperature measured at three locations went up, on average, 1.4 °C, and the JC08 mode warm-up resulted in 0.7 °C increase; the difference in the warm-up methods had little effect. Further, from the viewpoint of international discussions, similar comparisons were made with the WLTC mode. With the WLTC (Low+Middle+High) mode, the engine water temperature and the engine oil temperature became higher than in the JC08 mode warm-up, and lower than in the 60 km/h warm-up, but since these temperatures are stable, differences are considered insignificant. Because the battery temperature showed similar trends, it was understood that the WLTC mode warms up the vehicle better than the

JC08 mode. In addition, when the vehicle was kept running to *Extra High,* the ATF temperature, the front inverter temperature and the battery temperature showed a tendency to be higher than under other conditions.

Table 5.12 Differences in temperature before and after warming-up by different methods (testing vehicle C)

Warm-up conditions	Engine water temp.	Engine oil temp.	ATF temp.	Front inverter water temp.	Rear inverter water temp.	Battery surface temp. 1	Battery surface temp. 2	Battery surface temp. 3
60 km/h	61.5 °C	57.6 °C	34.5 °C	5.4 °C	9.8 °C	2.8 °C	0.9 °C	0.6 °C
JC08	58.3 °C	40.7 °C	16.3 °C	6.7 °C	8.0 °C	1.2 °C	0.5 °C	0.4 °C
WLTC (Low+Middle+High)	62.4 °C	52.9 °C	26.2 °C	3.7 °C	8.7 °C	2.4 °C	1.1 °C	1.0 °C
WLTC (Low+Middle+High+ Ex. High)	58.7 °C	66.6 °C	34.9 °C	9.0 °C	7.5 °C	3.3 °C	1.7 °C	1.5 °C

Next, Figure 5.52 shows effects of differences in temperature increase due to different warm-up methods on power output measurements. In terms of testing conditions, the vehicle speed was 160 km/h and the initial SOC was 90%. The axle-hub chassis dynamometer was used as the testing facility. To compare warm-up methods, the case where the vehicle was warmed up at the constant speed of 60 km/h was used as the standard and the cold condition and the JC08 mode warm-up were compared against it. The power outputs were compared in the wheel driving power, of which affecting factors included warm-up of the transmission, and in the total of the engine power output and the battery power, which is being proposed to the ISO.

In wheel driving power output, compared with the average value of 131.6 kW with the 60 km/h constant speed warm-up, that of the cold condition was 6.0 kW lower and the JC08 mode warm-up resulted in a value 1.2 kW higher. This showed that average values of power output were different by more than 1.0 kW, indicating that warm-up methods significantly affect power output measurements. Deviations were -0.7 to 0.6 kW with the 60 km/h constant speed warm-up, -0.8 to 0.5 kW under the cold conditions, and -1.0 to 0.7 kW in the JC08 mode; variations were not great.

When the power output was calculated by the method proposed to the ISO, which is to add the engine power output and the battery power, compared with the average value of 147.3 kW with the 60 km/h constant speed warm-up, that of the cold condition was 0.6 kW higher [sic.] and the JC08 mode warm-up resulted in a value 1.2 kW lower. This showed that average values of power output were different by more than 1.0 kW, indicating that warm-up methods somewhat affect power output measurements. Deviations were ±0.2 kW with the 60 km/h constant speed warm-up, -2.8 to 2.4 kW under the cold conditions, and -0.6 to 0.7 kW in the JC08 mode; measurements varied somewhat widely.

Further, power output measurements were compared between the two measuring locations: the method proposed to the ISO, which is to add the engine power output and the battery power to obtain upper-most stream measurements, and the wheel driving power output, which includes power loss in the transmission. In the wheel driving power output, obtained values were 21.1 kW lower under the cold conditions, 15.7 kW lower with the 60 km/h constant speed warm-up, and 13.3 kW lower in the JC08 mode warm-up. This revealed that in the calculation method proposed to the ISO, no warm-up method produced a widely different power output value, but in wheel driving power output

measurements, differences in warm-up methods resulted in differences in the warmed-up condition of the transmission and therefore affected power output measurements.

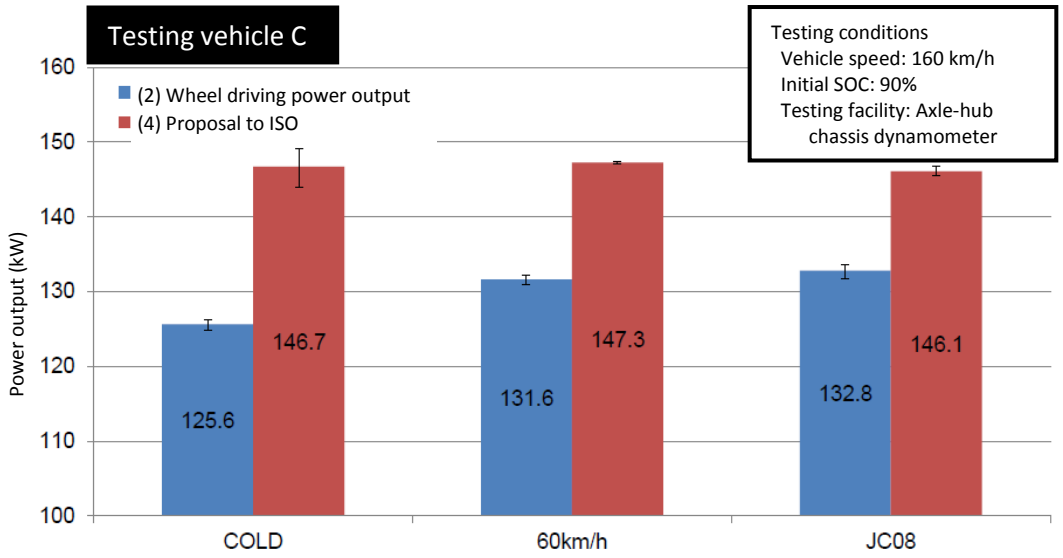

Figure 5.52 Effects of differences in temperature increase through different warm-up methods on power output measurements (testing vehicle C)

Figure 5.53 shows temperature at different locations at the time of maximum power output generation. The engine water temperature was 85.2 °C on average when the vehicle was warmed up at 60 km/h and under the cold condition, it was 31.2 °C on average, 54.0 °C lower. When the warm-up was done in the JC08 mode, it was 83.6 °C on average and 1.6 °C lower than that of the 60 km/h warm-up. The engine oil temperature showed the same tendencies; with the 60 km/h warm-up it was 90.7 °C on average, and the cold conditions resulted in 36.7 °C on average, 54.0 °C lower. When the warm-up was done in the JC08 mode, it was 83.3 °C on average and 7.4 °C lower than that of the 60 km/h warm-up. With regard to the temperature related to the engine, because, in the 60 km/h warm-up, the engine was running most of the time, variations in measurements such as the engine water temperature are small, but the JC08 mode warm-up showed wide variations in temperature relative to average values depending on the timing of the HEV operation because the engine repeatedly started and stopped during the warm-up. The ATF temperature was 65.4 °C on average when the vehicle was warmed up at 60 km/h, and under the cold condition, it was 31.7 °C, 33.7 °C lower. With the JC08 mode warm-up, it was 61.4 °C on average and 4.0 °C higher [sic.] compared with the temperature in the case of 60 km/h warm-up. The front inverter water temperature was 29.9 °C on average with the 60 km/h warm-up, and under the cold condition, it was 29.3 °C on averate, 0.6 °C lower. When the vehicle was warmed up in the JC08 mode, the average inverter temperature was 30.7 °C, 0.8 °C higher than that of the 60 km/h warm-up; little effects were observed. With regard to the battery temperature, when the vehicle was warmed up in the JC08 mode, the average of measurements taken at four locations was 27.0 °C, and it was 27.6 °C with the 60 km/h warm-up, 0.6 °C lower [sic.]. Under the cold condition, it was 27.4 °C on average and 0.4 °C lower [sic.] than the JC08 mode. The inverter cooling water temperature and battery surface showed little effects of different warm-up methods.